# Atmospheric regional climate projections for the Baltic Sea Region until 2100

Ole B. Christensen[1], Erik Kjellström[2], Christian Dieterich[3], Matthias Gröger[4], H.E. Markus Meier[4]

[1]Danish Meteorological Institute, Copenhagen, Denmark

5   [2]Swedish Meteorological and Hydrological Institute, Norrköping, Sweden

[3]Deceased

[4]Leibniz Institute for Baltic Sea Research Warnemünde, Rostock, Germany

*Correspondence to*: Ole B. Christensen (obc@dmi.dk)

**Abstract.** The Baltic Sea Region is very sensitive to climate change; it is a region with spatially varying climate and diverse
10   ecosystems, but also under pressure due to high population in large parts of the area. Climate change impacts could easily exacerbate other anthropogenic stressors such as biodiversity stress from society and eutrophication of the Baltic Sea considerably. Therefore, there has been a focus on estimations of future climate change and its impacts in recent research. In this review paper, we will concentrate on a presentation of recent climate projections from both atmosphere-only and coupled atmosphere-ocean regional climate models. The recent regional climate model projections strengthen the picture
15   from previous assessments. This includes a strong warming, in particular in the north in winter. Precipitation is projected to increase in the whole region apart from the southern half during summer. Consequently, the new results lend more credibility to estimates of uncertainties and robust features of future climate change. Furthermore, the larger number of scenarios gives opportunities to better address impacts of mitigation measures. The coupled atmosphere-ocean model locally modifies the climate change signal relative to that in the stand-alone atmosphere regional climate model. Differences are largest in areas
20   where the coupled system arrives at different sea-surface temperatures and sea-ice conditions.

## 1 Introduction

For many years, hundreds of global climate projections have been produced according to various scenarios of future greenhouse gas emissions and other forcing factors including changes in aerosols and land use. This has been coordinated in model inter-comparison projects (CMIPs), that have provided fundamental input to the Working Group I assessment reports
25   of the Intergovernmental Panel on Climate Change (IPCC; IPCC 2001, 2007, 2013). The fifth IPCC assessment report (AR5; IPCC 2013) was built on the World Climate Research Programme's (WCRP) Coupled Model Intercomparison Project phase 5 (CMIP5) multi-model data (Taylor et al., 2012). Many general circulation models (GCMs) participated in simulations according to several Representative Concentration Pathway (RCP) scenarios (van Vuuren et al., 2011).

The Baltic Sea Region is highly diverse with considerable spatial variability over small distances compared to typical GCM
resolutions. Consequently, GCMs do not represent all relevant processes at adequate scales and results are often biased (e.g.
Graham et al., 2008). High-resolution regional climate models, nested in the GCMs, have been shown to add value to the
GCM results and to promote detailed analysis on regional to local scales (e.g. Giorgi and Gao, 2018). At the European level,
considerable efforts have therefore been undertaken to downscale GCM simulations to a higher horizontal resolution with
RCMs. The history of coordinated RCM simulations started in the PRUDENCE project with RCMs mostly operated at 50
km spatial resolution (Christensen and Christensen 2007), continued with the ENSEMBLES project (van der Linden and
Mitchell 2009;. Hanel and Buishand 2011; Kyselý et al. 2011; Räisänen and Eklund 2011; Déqué et al. 2012; Kjellström et
al. 2013) and more recently in the Euro-CORDEX initiative, which forms part of the Coordinated Regional climate
Downscaling EXperiment (CORDEX, **www.cordex.org**; e.g. Jacob et al., 2013; Kotlarski et al., 2014; Keuler et al., 2016;
Kjellström et al., 2018). Most recently, the European Copernicus Climate Change Services has supported an extension of the
available CMIP5-driven RCM downscaling simulations in the Euro-CORDEX setup with around 12 km spatial resolution
(Vautard et al., 2021; Coppola et al., 2021). This has led to the public availability of a large amount, currently 127, different
simulations following the RCP2.6, RCP4.5, and RCP8.5 scenarios (some simulations with known errors are not counted).

Regional climate models have been used not only for downscaling of climate change scenarios. Also, observation-based
reanalysis datasets have been extensively downscaled with RCMs in recent years (e.g. Feser et al. 2001; Hagemann et al.
2004; Christensen et al. 2010; Samuelsson et al. 2011; Kotlarski et al., 2014; Prein et al., 2015). These experiments are
useful for comparing RCM results and observational data for recent decades, and thereby for evaluation of RCM models.
The RCMs are found to capture many features of the climate in a realistic way albeit with some systematic errors and biases
(Wibig et al., 2015; Kjellström and Christensen, 2020). As a remedy, bias-correction is sometimes applied to the results (e.g.
Dosio et al., 2016). Biases are generally larger when GCMs are downscaled as these show systematic biases in their
representation of the atmospheric circulation at large scales, of temperature, humidity and sea surface conditions. For an area
like the Baltic Sea region, this implies that sea surface temperatures (SSTs) and sea ice from the coarse-scale driving GCM
may not be completely adequate as input to an RCM; this constitutes an additional source of potential uncertainty of the
downscaled regional scenarios (Kjellström and Ruosteenoja, 2007).

During the past decades a number of regional coupled atmosphere-ocean-sea-ice models with focus on the Baltic Sea and
adjacent marginal seas have therefore been developed for climate studies (e.g. Gustafsson et al., 1998; Döscher et al., 2002;
Wang et al., 2015; Dieterich et al., 2019; Primo et al., 2019; Kelemen et al., 2019; Akhtar et al., 2019; Sein et al., 2020). In
these models, prescribed boundary conditions at the sea surface (i.e. sea ice and sea surface temperature (SST)) were
replaced by online coupled ocean models allowing for a direct and more realistic representation of air-sea thermal feedback
mechanisms (see review by Gröger et al., 2021b). These coupled models exhibit a different model solution for many climate
variables compared to their atmosphere stand-alone counterparts, especially over the coupled region (Gröger et al., 2015;
Ho-Hagemann et al., 2017; Primo et al., 2019; Gröger et al., 2019, 2020). The most recent and largest ensemble of regional coupled climate change simulations was provided by Dieterich et al. (2019) and Gröger et al. (2019, 2020) and is based on the regional climate model RCA4 coupled interactively to the ocean model NEMO.

Available RCM literature describes extensive studies of possible future climate conditions for many areas, including the Baltic Sea basin (see, e.g., Lind and Kjellström 2008; Kjellström and Lind 2009; Benestad 2011; Kjellström et al. 2011a; Nikulin et al. 2011; Christensen et al. 2015; Christensen and Kjellström 2018; Coppola et al., 2021). Ensembles of climate projection simulations have been used to obtain probabilistic climate change information, both GCM (Lind and Kjellström 2008; Räisänen 2010) and RCM ensembles (Buser et al. 2010; Donat et al. 2011). In addition, the wider range of GCM scenarios has been used to set regional scenarios in a broader context (Lind and Kjellström 2008; Kjellström et al., 2016 and 2018).

This work aims at presenting climate change in the area around the Baltic Sea, as it is projected by the very large ensemble of Euro-CORDEX RCMs at 12 km resolution. The spread in results between the projections is used to discuss uncertainties in future climate change. In addition to the uncoupled atmosphere-only EURO-CORDEX RCM ensemble, we will also assess changes in an ensemble with the atmospheric regional model RCA4 coupled to the NEMO ocean model. A comparison between results from the stand-alone atmospheric model and the coupled model provides input to the assessment of uncertainties in future climate change projections for the area.

## 2. Data and methods

The main results of this study build on seasonal means from the publicly available and accessible EURO-CORDEX data, which at the time of writing consisted of the 124 simulations indicated in Tab. 1 out of a current total of 127. We will focus on data of the most commonly studied fields: surface air temperature, average total precipitation, mean wind speed at 10 m height, incoming short-wave radiation, and average winter snow and sea-ice cover.

The consequences of extreme weather events impact many aspects of society. Extreme precipitation often results in flooding, which often causes extensive damage as do extreme winds in connection with low-pressure systems. Changes in these extremes as a result of anthropogenic climate change have received considerable attention. We will therefore also report on extremes of daily precipitation and 10 m wind speed.

Not all simulations have been analysed for extremes; two WRF361H simulations do not contain solar radiation; and snow and sea ice from several simulations either do not exist in the archive or have not been downloaded. Some simulations with crCLIM are missing DJF 2005-2006 due to a problem when handling the transition between historical and scenario simulations; we have repeated DJF 2004-2005 in its place. All simulations driven by HadGEM2-ES are missing the year 2100; for these simulations we have used 2070-2099 as the end-of-century period.

The second BACC report from 2015 (BACC II Author Team, 2015) showed similar maps to those presented here. These results were based on the ENSEMBLES database (van der Linden and Mitchell, 2009), consisting of simulations following the SRES (Nakićenović et al., 2000) A1B scenario performed in 25 km grid resolution. The periods compared were 1961-1990 and 2071-2100. The mean GCM global temperature change, weighted with the number of RCM simulations in the ensemble, for the EURO-CORDEX and ENSEMBLES simulations can be seen in Tab. 2. Note that the reference periods for ENSEMBLES are 1961-1990 and 2071-2100, whereas they are 1981-2010, 2041-2070 and 2071-2100 for EURO-CORDEX.

To a high extent, maps over the Baltic Sea catchment of climate change for the weaker emission scenarios exhibit the same patterns as the RCP8.5 climate change normalized by global temperature change; maps are available in the Supplementary Material. The weighted global warming between the relevant periods for the simulations in BACC II, driven by the SRES A1B emission scenario, is 3.00 degrees.

| RCP8.5 | RCA4 | CCLM4-8-17 | crCLIM | REMO 09,15 | RACMO22E | HIRHAM5 | WRF361H | WRF381P | ALADIN63 | RegCM4.6.1 | HadREM3-GA7.05 | Total by GCM |
|---|---|---|---|---|---|---|---|---|---|---|---|---|
| MOHC-HadGEM2-ES | 1 | 1 | 1 | 1 | 1 | 1 | 1 | 1 | 1 | 1 | 1 | 11 |
| ICHEC-EC-EARTH | 3 | 1 | 3 | 3 | 3 | 3 | 1 | 1 | | 1 | 1 | 18 |
| CNRM-CERFACS-CNRM-CM5 | | | 1 | 1 | 1 | 1 | | 1 | 1 | | 1 | 7 |
| NCC-NorESM1-M | 1 | | 1 | 1 | 1 | 1 | | 1 | 1 | 1 | 1 | 9 |
| MPI-M-MPI-ESM-LR | 3 | 1 | 3 | 3 | 1 | 1 | 1 | 1 | 1 | 1 | 1 | 17 |
| IPSL-IPSL-CM5A-MR | 1 | | | 1 | | | | 1 | | | | 5 |
| CCCma-CanESM2 | | 1 | | 1 | | | | | | | | 2 |
| MIROC-MIROC5 | | 1 | | 1 | | | 1 | | | | | 3 |
| Total by RCM | 9 | 5 | 9 | 10 | 8 | 8 | 4 | 6 | 4 | 4 | 5 | 72 |
| RCP4.5 | RCA4 | CCLM4-8-17 | crCLIM | REMO 09,15 | RACMO22E | HIRHAM5 | WRF361H | WRF381P | ALADIN63 | RegCM4.6.1 | HadREM3-GA7.05 | Total now |
| MOHC-HadGEM2-ES | 1 | 1 | | 1 | 1 | 1 | | | | | | 5 |
| ICHEC-EC-EARTH | 1 | 1 | | 1 | 2 | 1 | | | | | | 6 |
| CNRM-CERFACS-CNRM-CM5 | | | | | 1 | | | | 1 | | | 2 |
| NCC-NorESM1-M | 1 | | | 1 | | 1 | | | | | | 3 |
| MPI-M-MPI-ESM-LR | 1 | 1 | | 2 | | | | | | | | 4 |
| IPSL-IPSL-CM5A-MR | 1 | | | | | | | 1 | | | | 2 |
| Total by RCM | 5 | 3 | | 5 | 4 | 3 | | 1 | 1 | | | 22 |
| RCP2.6 | RCA4 | CCLM4-8-17 | crCLIM | REMO 09,15 | RACMO22E | HIRHAM5 | WRF361H | WRF381P | ALADIN63 | RegCM4.6.1 | HadREM3-GA7.05 | Total now |
| MOHC-HadGEM2-ES | 1 | | | 1 | 1 | 1 | | | | 1 | 1 | 6 |
| ICHEC-EC-EARTH | 1 | 1 | | 1 | 1 | 1 | | | | | 1 | 6 |
| CNRM-CERFACS-CNRM-CM5 | | | | 1 | 1 | | | | 1 | | | 3 |
| NCC-NorESM1-M | 1 | | | 1 | 1 | | | | | 1 | | 4 |
| MPI-M-MPI-ESM-LR | 1 | 1 | | 2 | 1 | | 1 | | | 1 | | 7 |
| IPSL-IPSL-CM5A-LR | | | | 1 | | | | | | | | 1 |
| NOAA-GFDL-ESM2G | | | | 1 | | | | | | | | 1 |
| MIROC-MIROC5 | | 1 | | 1 | | | | | | | | 2 |
| Total by RCM | 4 | 3 | | 9 | 5 | 2 | 1 | | 1 | 3 | 2 | 30 |
| Grand total by GCM | 18 | 11 | 9 | 24 | 17 | 13 | 5 | 7 | 6 | 7 | 7 | 124 |

Table 1. Model simulations of the study. These constitute the entire set of seasonal-average fields available from the Earth System Grid Federation archive (ESGF; http://esgf-data.dkrz.de) in May 2021. There are 72 ensemble members following RCP8.5, 22 following RCP4.5, and 30 following RCP2.6.

| Project | Scenario | Ensemble size | Mid-century warming | End-century warming |
|---|---|---|---|---|
| ENSEMBLES | SRES A1B | 13 | - | 3.00 |
| EURO-CORDEX | RCP8.5 | 72 | 2.21 | 3.71 |
| EURO-CORDEX | RCP4.5 | 22 | 1.67 | 2.13 |
| EURO-CORDEX | RCP2.6 | 30 | 1.22 | 1.19 |

**Table 2** Average global warming from driving GCMs in each scenario, weighted by the number of downscaling simulations of each.

Three different emission scenarios have been widely used for downscaling within CORDEX. The RCP2.6 scenario is the most moderate and will require a targeted emission reduction worldwide. The RCP8.5 scenario, in contrast, is consistent with large future increases in emissions, little emission mitigation, and a continued reliance on fossil fuels for many years. In the middle, the RCP4.5 scenario requires a considerable amount of mitigation, but is very unlikely to achieve the 2-degree warming limit relative to pre-industrial conditions, which the Paris agreement targets.

In this study we will concentrate on the warmer RCP8.5 scenario. The maps below show results based on 72 regional climate change simulations from the RCP8.5 EURO-CORDEX simulations listed in Tab. 1. Corresponding plots for other scenarios and periods can be found in the Supplementary Material. For each location, the median among ensemble members of the change is shown together with the first and third quartiles. In the maps showing the median we only display grid points where 75% of models agree on the sign, i.e., where both quartile plots show the same sign, elsewhere we indicate by white colour that the changes are not robust. We will discuss only winter (DJF) and summer (JJA) in this study. The scatter plots below show results for all simulations following the three commonly used scenarios (Tab. 1). Where possible we also include results from the ENSEMBLES project, which were the basis of BACC II (Christensen et al., 2015). In addition to the average over the entire Baltic Sea catchment region including the Baltic Sea, we divide the region into sea points and land points north and south of 60N. In the Supplementary Material, Tab. S1-S20, tables of ensemble means and ensemble

standard deviations can be found for temperature and precipitation, for both periods, all scenarios (including the BACC II/ENSEMBLES SRES A1B scenario), and all five areas.

125 We will also investigate the coupled model ensemble with RCA4-NEMO. RCA4 is set up for the EURO-CORDEX domain with a horizontal resolution of ~25 km and 40 vertical levels. NEMO simulates the hydrodynamics of the Baltic Sea as well as the North Sea at ~3.7 km resolution and 56 vertical levels (Gröger et al., 2015; Dieterich et al., 2019). Air-sea fluxes are exchanged every three hours between the ocean and the atmosphere. The RCA4-NEMO ensemble consists of 22 downscaled GCM simulations based on 8 different global models as well as a reanalysis for the historical period and the RCP2.6,
130 RCP4.5, and RCP8.5 scenarios.

These results will be compared to the corresponding RCA4 atmosphere-only simulations, which can be found in the EURO-CORDEX archive. When possible, these simulations are included into the scatter plots below.

## 3. Results and discussion

### 3.1. Temperature

135 According to the analysed EURO-CORDEX ensemble, we will see increasing air temperature in the Baltic Sea area during the present century. According to this ensemble it is a robust result for all seasons, locations, simulations and scenarios.

For both seasons analysed, the temperature change shows spatial gradients with the strongest warming in the north-east (Figure 1). Winter warming is larger than summer warming, and larger than the global average warming of about 3.7 degrees (Tab. 2); in the north-east it approaches twice the global average warming. Higher warming than the global average is
140 generally expected for land areas, since land heats more quickly than sea. The strong winter increase is also influenced by the feedback mechanisms involving retreating snow and sea-ice. There is a general pattern of higher warming in the north than in the south, but there is a spread in the magnitude of the change. This is illustrated in the columns of the figures below. As only 8 GCMs have been used for these RCP8.5 RCM experiments, the spread between quartiles is lower than what would have come from an exhaustive downscaling of all CMIP5 global simulations.

145 Earlier studies have shown that the increase in winter temperatures is strongest for the coldest episodes (Kjellström 2004) as well as for extreme daily maximum and minimum temperatures (Kjellström et al. 2007; Nikulin et al. 2011). There is a significant decrease in the probability of cold temperatures (Benestad 2011). Warm summer extremes are projected to become more pronounced; for example, Nikulin et al. (2011) an ensemble of six RCM simulations, all downscaling GCMs under the SRES A1B scenario, and showed that warm extremes with a present-day (1961–1990) return period of 20 years
150 will be reached four times as often in Scandinavia by 2071–2100, with a frequency around once every five years .

Summer warming in the Baltic Sea basin is smaller than winter warming, and it is relatively homogeneous across the area. A tendency is seen for larger warming over land areas in the northernmost parts of the Baltic Sea basin. These areas are closest to the northern rim of Scandinavia and the Kola Peninsula where warming in summer is as high as that projected for parts of southernmost Europe (Kjellström et al., 2018). The most extreme summer warming is comparatively larger than the median

155    in the south-eastern part of the region. This is related to the large-scale pattern of warming in Europe, where the strongest summer warming is seen in southern Europe. In the north-eastern part of the region, a large warming may be related to the ice-albedo feedback mechanism. Similar results for other GCM/RCM combinations have been reached in, e.g., Christensen and Christensen (2007), Kjellström et al. (2011a), and Vautard et al. (2014). These results are consistent with results for 2021–2050 in Déqué et al. (2012). This study finds that there is a significant temperature response, even for the relatively

160    short-term 2021–2050 time frame, even though the total uncertainty related to the choice of model combination (GCM/RCM) and sampling (natural variability) is large,. Similarly, Kjellström et al. (2013) showed early emergence already in the first few decades of the 21st century of trends in temperature despite large natural variability as represented in the ENSEMBLES RCM projections used in BACCII.

Corresponding changes in the daily minimum temperature and daily maximum temperature (not shown) have the same

165    patterns as the average temperature change, with the expected larger magnitude of warming for minimum temperature. This is a direct consequence of the fact that the greenhouse effect acts by reducing outgoing long-wave radiation, which acts to cool the surface particularly when the ground is warmer than the air, e.g., during winter and during nights.
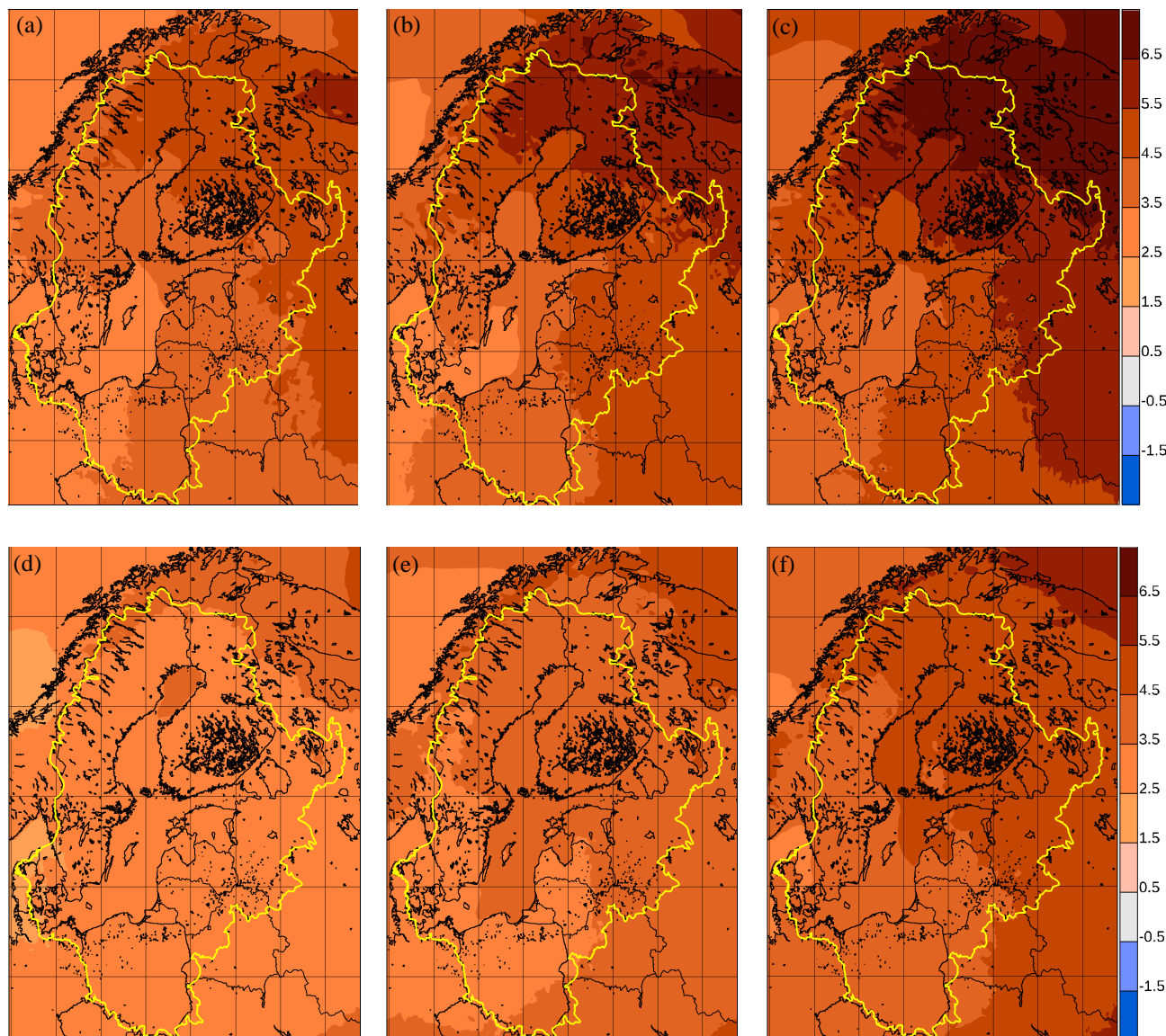
**Figure 1.** Temperature change between 1981-2010 and 2071-2100 for 72 simulations from Euro-CORDEX according to the
170  RCP8.5 scenario. Panels a-c: winter. Panels d-e: summer. Panels a,d: lowest quartile; Panels b,e: median value; Panels c,f:
higher quartile. In all following figures, the mid column depicting pointwise median values is only coloured when 75% of
the simulations agree on the sign of the change. The Baltic Sea Catchment is indicated in yellow.

## 3.2 Precipitation

The multi-model EURO-CORDEX ensemble relative precipitation change for winter and summer is shown in Fig. 2. The
175  ensemble is the same as in Fig 1.

During winter, the relative increases are quite homogeneous, although there are large differences between the lower and upper quartiles. These differences are largest west of the Baltic Sea catchment (Norway) as a result of different changes in the large-scale circulation. For summer there is a clear pattern of more positive change in the north versus less positive change in the south. As expected, winter increases are projected to be larger in winter than in summer. Roughly, the winter

180    increase is 25-35% over most of the area in the median, and the summer increase is 15-25% for the northern part of the area. This is consistent with the AR5 Climate Atlas, where median increases of precipitation in the area are 10-20% for the winter half year and 5-10% for summer, as these results correspond to the RCP4.5 scenario with around 2.5 degrees of warming for the periods mapped, whereas the Euro-CORDEX results correspond to a global warming of 3.8 degrees.

For summer there is disagreement on the sign of climate change for most of the southern half of the area, indicated by the

185    masked-out area defined as regions where at least 25% of the models disagree on the sign with the majority. Since the period mapped here consists of the three summer months June-August, whereas the AR5 Climate Atlas maps April-September, a comparison of the position of the no-change area is difficult. In an analysis of the older ENSEMBLES simulations (Déqué et al., 2012) almost all land points in the Baltic Sea region showed significantly positive summer precipitation signals.

This general picture of change is not surprising. Climate models generally project the global hydrological cycle to become

190    more intense (e.g. Held and Soden 2006). For Europe this corresponds to increasing precipitation in northern Europe and decreasing precipitation in southern Europe, both in winter and summer (Christensen et al. 2007). Between these areas of projected increase and projected decrease, only small changes or changes in different directions are projected (see e.g. Kjellström et al. 2011a). The location of the transition zone depends on the season and is located farther to the south in winter than in summer. In summer, this zone shifts into the Baltic Basin: winter precipitation is projected to increase over the

195    entire Baltic Sea catchment, while summer precipitation is mostly projected to only increase in the northern half of the basin. In the south, precipitation change is small for the ensemble mean, and there is a large spread between different models with both increases and decreases. Basically, both increases and decreases are possible in the future.
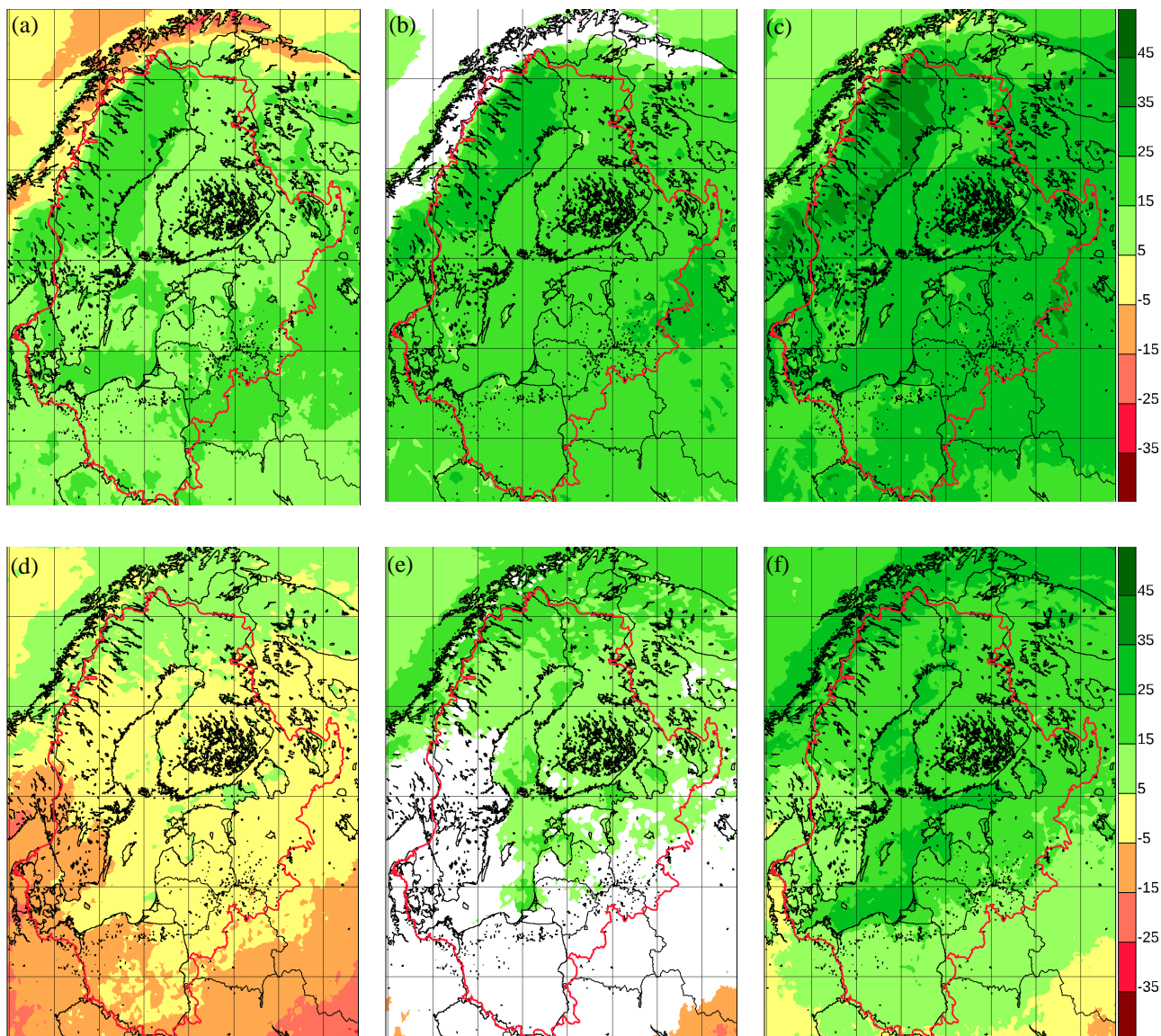
**Figure 2**. Precipitation relative change (%) between 1981-2010 and 2071-2100 for 72 simulations from Euro-CORDEX
according to the RCP8.5 scenario. a-c: winter; d-e: summer. a,d: lowest quartile; b,e: median value; c,f: higher quartile. In all
following figures, the mid column depicting pointwise median values is only coloured when 75% of simulations agree on the
sign of the change. The Baltic Sea catchment is indicated in red.

In Fig. 3 we show scatter plots, where the change between 1981-2010 and 2071-2100 of precipitation is plotted against the
corresponding relative change of temperature for each model and each scenario. Ensemble means for the three scenarios are
indicated by the three larger symbols. This calculation has been performed for various subsets of the Baltic Sea catchment

(see Fig. 1): The entire catchment; only land points; only sea points; only land points north and south of 60 degrees north, respectively.

There is a strong correlation between temperature and precipitation in winter with significant regression slopes of around 5 percentage points per degree and correlation coefficients of 0.5 to 0.6 depending on the sub-area. This is an indication of an approximate common sensitivity of precipitation change to local temperature change. This correspondence breaks down for summer, where the plots contain much more noise, indicating large model-dependent influences on the precipitation signal. The north-south gradient in summer precipitation change is apparent in the model averages (compare the northern and southern land point plots), but the inter-model spread is large.

Due to the roughly 20% higher average global warming in the current RCP8.5 ensemble than in the GCMs underlying BACC II (see Tab. 2), we would have expected general climate change to be around 20% larger for EURO-CORDEX RCP8.5 than those presented in BACC II. It is noteworthy that this difference is not seen in Fig. 3, where we have plotted temperature and precipitation change for the BACC II simulations (BACC II Author Team, 2015)) along with the three scenarios of the present analysis. The BACC II results correspond to the RCP8.5 results both with respect to temperature and precipitation change.
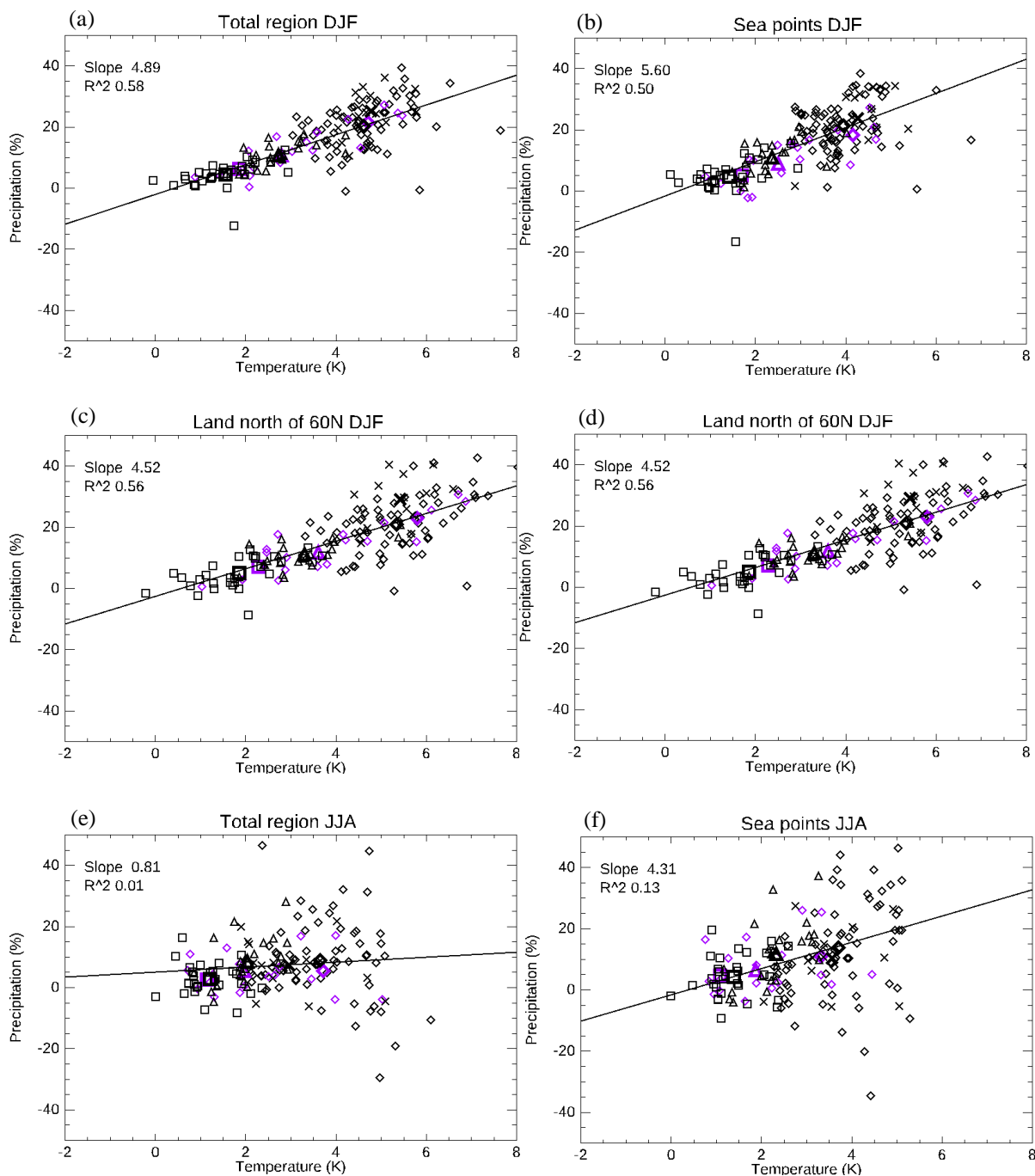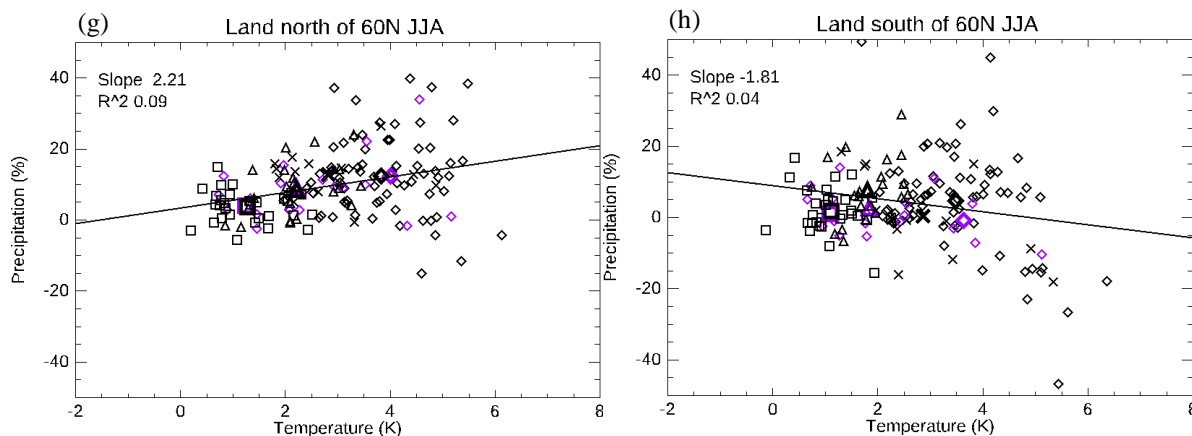
**Figure 3** Relative change 1981-2010 to 2071-2100 of precipitation against temperature change for individual models and all scenarios. Scenario means are indicated by larger symbols. Squares: RCP2.6; Triangles: RCP4.5; Diamonds: RCP8.5; Crosses: The ENSEMBLES simulations analysed in BACC II (2015). Purple colour: The RCA4-NEMO atmosphere-ocean coupled simulations. Calculation performed for subsets of the Baltic Catchment: The entire catchment; sea points; land points north and south of 60 degrees north, respectively. Panels a-d show winter; panels e-h show summer. The lines, with quoted slope and squared correlation coefficient, are best fits to all EURO-CORDEX and ENSEMBLES data, but do not include coupled-model results.

## 3.3 Extreme precipitation

The water-holding capacity of the atmosphere increases with increasing temperature. Therefore precipitation extremes are projected to increase with climate warming (e.g. Lenderink and van Meijgaard 2010). Several studies, some of which are described in the following, indicate that extreme precipitation is likely to increase in the future, even in areas and seasons, where the average precipitation does not increase. One example is the IPCC Special Report on Extreme events (Seneviratne et al., 2012) where it was shown that higher extremes of precipitation consistently show larger increases than lower extremes, and higher increases than averages.

Already simulations from the PRUDENCE project (Christensen and Christensen, 2003) showing a considerable decrease in average summer precipitation in large parts of southern Europe at the same time showed an increased probability of very extreme precipitation in that area as well as in the north, where average precipitation was not projected to decrease. Quite generally, more intense precipitation can be expected on all time scales, from single rain showers to synoptic-scale precipitation.

Nikulin et al. (2011) investigated an ensemble of RCM simulations following the SRES A1B scenario with the RCA model; they showed that the 20-year return value of precipitation extremes in Scandinavia in the period 1961–1990 was projected to

decrease to 6–10 years in 2071–2100 for summer over northern Europe and to 2-4 years in winter. Similarly, Larsen et al. (2009) analysed a high-resolution RCM integration and reported that the return period for 20-year rainfall events at hourly duration decreased to about 4 years for Sweden..

250 Collected results from 90 of the models from the Euro-CORDEX project are illustrated in Fig. 4, along with results from the coupled models discussed below. For data availability reasons at the time of writing, not all simulations have been analysed for extreme precipitation. We will here use the 10-year return value as representative of extreme precipitation. This is the daily precipitation amount so large that it is only exceeded every 10 years for a long-term average. The model-median signal has a consistently positive sign across the domain for the areas where more than 75% of the model results have the same sign. The temperature dependence of the increases in the Baltic Sea basin (slopes in Fig. 4) aregenerally larger in summer

255 than in winter with the southern land points as an exception, the same area where the average precipitation (Figs 2-3) decreases. The inter-model spread is considerably larger in summer than in winter, illustrating the greater influence of local processes in this season; it should be noted that the increase in the number of models analysed, compared to Christensen and Kjellström (2018) from 19 to 90 results in a considerably more robust positive signal in the summer 10-year return value.

The relative change of extreme precipitation in winter (Fig. 4 upper panels) are quite similar to the relative change in average
260 precipitation (Fig. 2), indicating no change in the shape of the intensity distribution function. For summer, however, the projected change in extreme precipitation is consistently more positive than the change in average precipitation. While the temperature sensitivity (slopes in Figs 3 and 4) for winter average precipitation and winter extreme precipitation are almost identical, the sensitivity of extremes in summer is larger than for winter, while it is insignificant for the average precipitation in summer. This feature is, however, less apparent in the Euro-CORDEX results than in the PRUDENCE results of BACC
265 (BACC Author Team, 2008) and the ENSEMBLES results described in BACC II (BACC II Author Team, 2015). It is not clear if this difference is due to the fact that the RCMs are run at different horizontal resolutions in the three projects (i.e. 50, 25 and 12.5 km, respectively) or if it is a consequence of different model formulations in the projects, or of the large-scale climate change signal as imposed by the underlying GCMs that also differs between the experiments.

Recently, several research institutes have started employing convection permitting regional models (CPMs). Such models are
270 able to run in much higher resolution, since they avoid the possible double counting, where traditional hydrostatic RCMs with fully parameterized convective precipitation release may produce convective precipitation explicitly as well as parameterized. With CPMs grid distances below the "grey zone" of 3-5 km are possible. In Lind et al. (2020) results are presented with the CPM HARMONIE-Climate (HCLIM), produced in a common Nordic model collaboration (NorCP) with participation from Sweden, Norway, Denmark, and Finland. Comparing a CPM version of HCLIM in 3 km resolution with a
275 non-CPM version in 12 km, it was concluded that the high-resolution model showed better results for precipitation intensity distribution, including extreme precipitation at sub-daily time scales, for the summer precipitation diurnal cycle, and for snow in mountains.

Based on convection-permitting models it has been argued that changes in precipitation extremes of a shorter duration may be larger than those for longer time scales (e.g. Kendon et al. (2014), Lenderink and van Meijgaard (2010)). However, other results indicate (Ban et al., 2014) that convection-permitting models may give roughly the same increase also for shorter durations, consistent with the Clausius-Clapeyron scaling of around 6-7% per degree of warming. In a study of idealized warming experiments repeating present-day observed weather under warmer and moisture conditions with the HCLIM model, Lenderink et al (2019) showed that there is a strong dependence on moisture availability to the increase in the precipitation extremes.

In Christensen et al. (2019) a thorough comparison of change patterns of mean temperature and precipitation has been performed for the PRUDENCE simulations behind the first BACC report (BACC Author Team, 2008), the ENSEMBLES simulations behind the second report (BACC II Author Team, 2015), and the EURO-CORDEX data behind the present report. This analysis used patterns of change scaled with global temperature change and is therefore useful for pinpointing differences between the BACC reports extraneous to the variations of general scenario strength, i.e., differences in local sensitivity and/or change patterns apart from those due to differences in emission scenarios. The most important differences between BACC II and the current simulations are a slightly reduced winter warming per unit of global warming; a smaller wintertime precipitation increase, but a slightly larger increase of summer precipitation over the Baltic Sea. These conclusions do not contradict the results from Fig. 3, since a scaling with global warming would increase both local precipitation and local temperature changes for the BACC II ENSEMBLES results relative to RCP8.5.
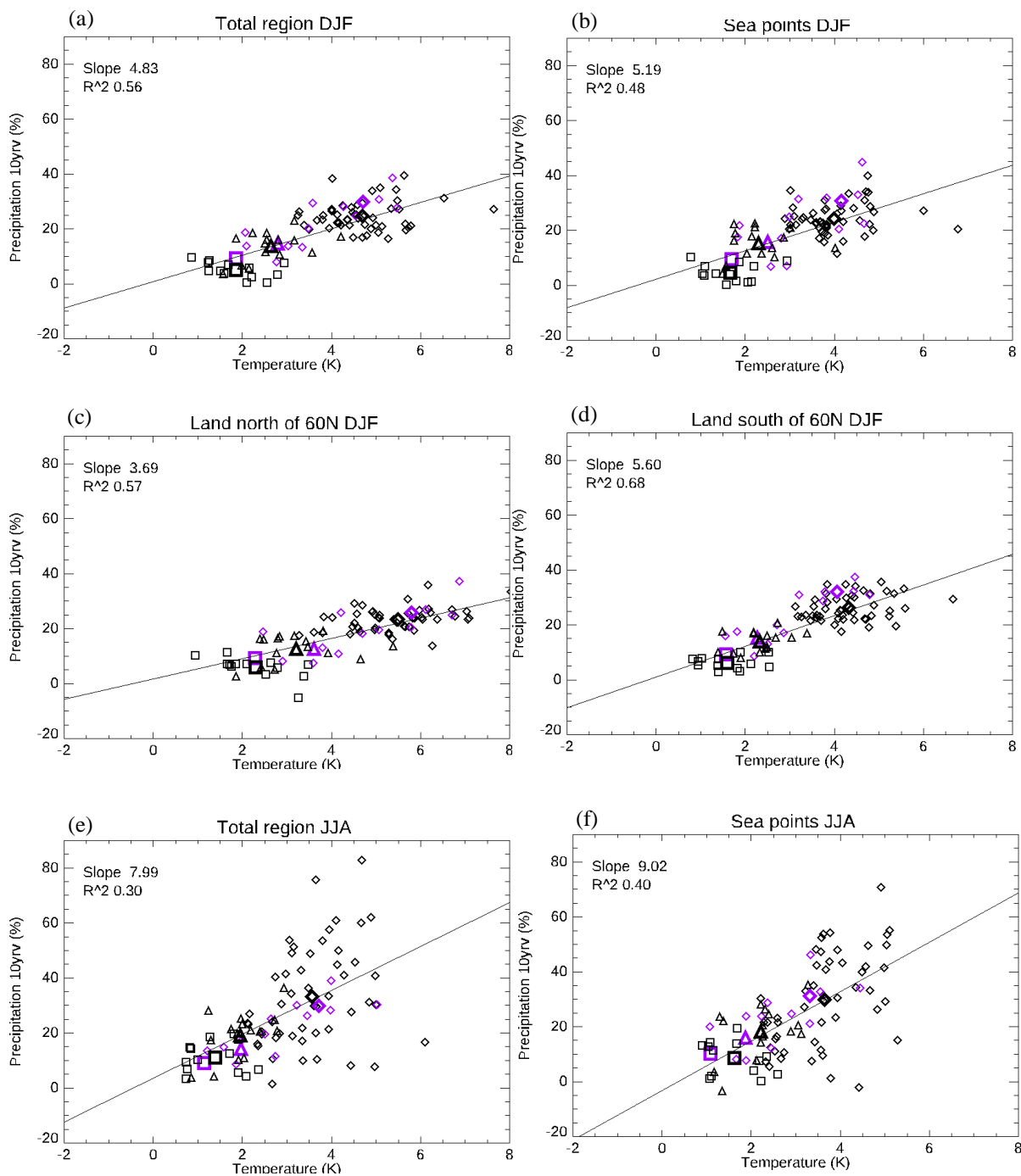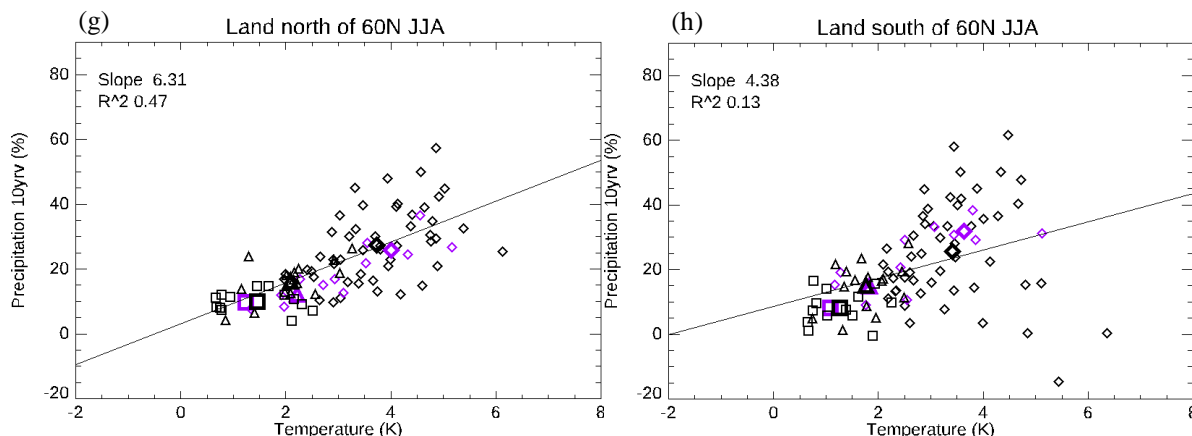
**Figure 4** Relative change 1981-2010 to 2071-2100 of the 10-year return value of daily precipitation against temperature change for individual models and all scenarios. Scenario means are indicated by larger symbols. Squares: RCP2.6; Triangles: RCP4.5; Diamonds: RCP8.5. Purple colour: The RCA4-NEMO atmosphere-ocean coupled simulations. Calculation performed for subsets of the Baltic Catchment: The entire catchment; sea points; land points north and south of 60 degrees north, respectively. Panels a-d show winter; panels e-h show summer. The lines, with quoted slope and squared correlation coefficient are best fits to all EURO-CORDEX data.

### 3.4 Wind speed

Changes in the climatology of 10-metre wind speed is even more uncertain than it is the case for the precipitation climate, both for seasonal mean conditions and for extremes on shorter time scales (e.g. Kjellström et al. 2011a; Kjellström et al. 2018; Nikulin et al. 2011).

In a study by Donat et al. (2011) of annual 98th percentile daily maximum wind speed change in RCM simulations from the ENSEMBLES project, for the middle of the  century as well as the end of the century. The ensemble average, like the driving GCMs, increased in a region from the British Isles to the Baltic Sea, and a decreased in the Mediterranean area. Nikulin et al. (2011) found increasing wind speed extremes (20-year return periods of annual maximum 10-metre wind speed) over the Baltic Sea in five out of six simulations, based on an ensemble of one RCM downscaling six different GCMs under the A1B scenario,.

In BACC II (BACC II Author Team, 2015), an analysis of 13 ENSEMBLES simulations showed a very small insignificant median increase in the southern part of the Baltic Sea area; the signal is consistent with the findings by Donat et al. (2011), but with a large spread between models.

Figure 5 shows average changes over the Baltic Sea for the 72 Euro-CORDEX RCP8.5 simulations, the 22 RCP4.5
320   simulations, and the 30 RCP2.6 simulations, which are used (Tab. 1). There is very little agreement between the models
about even the direction of change for winter in the Baltic Sea area unlike the tendency for reduced average wind speed
outside of the study area over the North Atlantic (not shown). Over the northernmost parts of the Baltic Sea basin, the
Bothnian Bay, there is an indication of larger wind speed increase (or less decrease) over the sea than over surrounding land
areas. This feature has previously been pointed out by Kjellström et al. (2011a), Meier et al. (2011) and Tobin et al (2016)
325   and has been related to decreases in sea-ice in the future warmer climate leading to consequent changes in stability
conditions of the lower atmosphere. See also the comparison between regional coupled and uncoupled simulations in Fig. 15
where the, probably more consistent, treatment of ice-albedo feedback leads to a slightly larger increase in winter. As seen in
Fig. 5 panel 2, the slight increase in mean wind over the southern part of the Baltic Sea in BACC II is not projected in the
current simulations.

330   Summer results show consistent but small reductions of wind over land of about 2-6%. Again, in summer, there are
differences between land and ocean areas with generally larger increases, or smaller decreases, over the Baltic Sea than its
surrounding land areas.
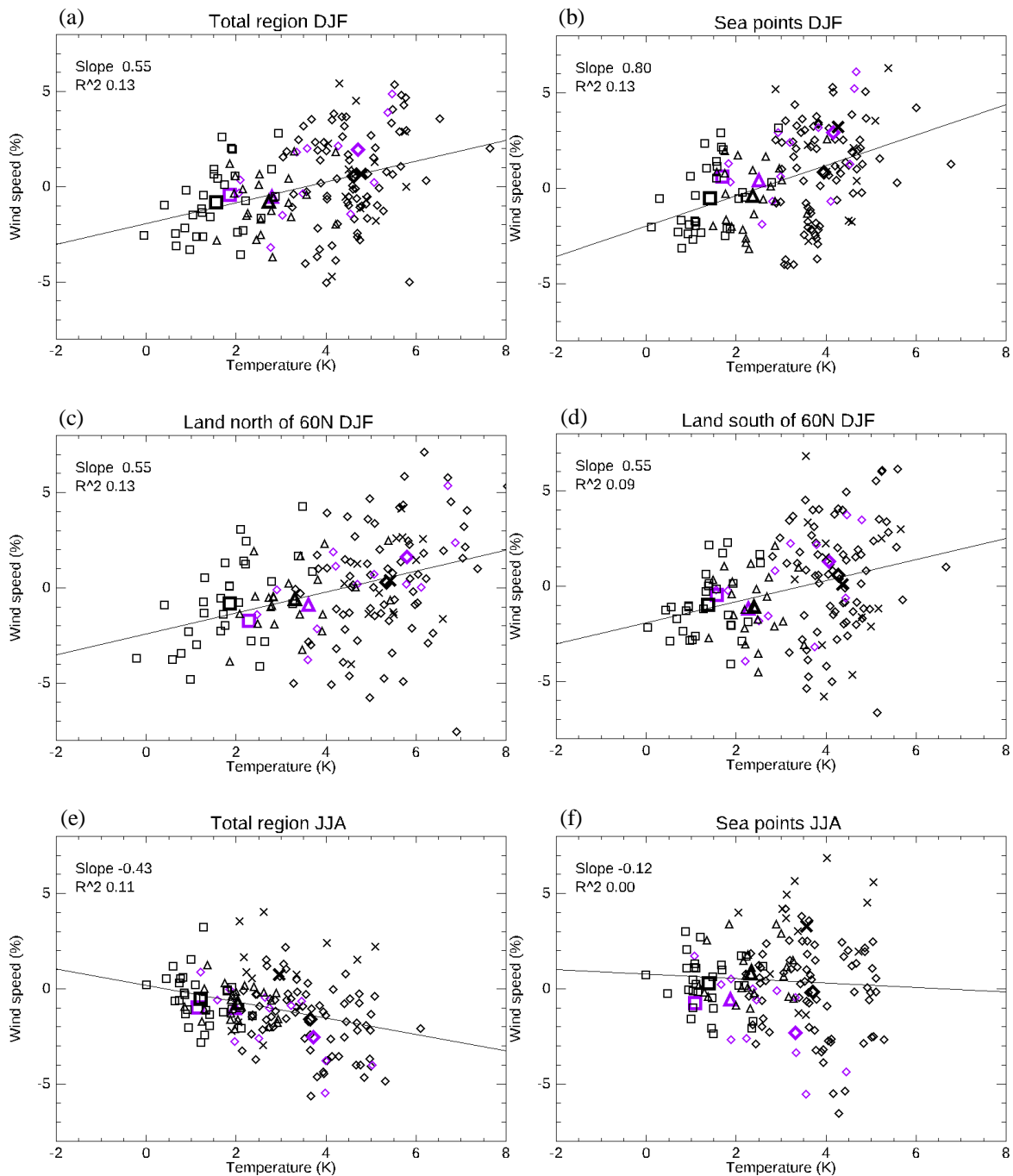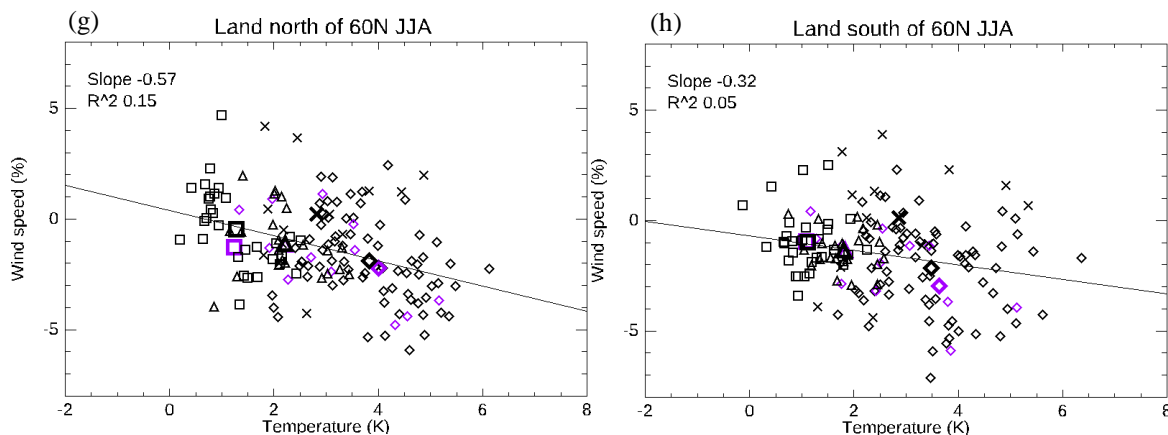
**Figure 5** Relative change 1981-2010 to 2071-2100 of 10m wind speed against temperature change for individual models and all scenarios. Scenario means are indicated by larger symbols. Squares: RCP2.6; Triangles: RCP4.5; Diamonds: RCP8.5.

340   Crosses: The ENSEMBLES simulations analysed in BACC II (BACC II Author Team, 2015). Purple colour: The RCA4-NEMO atmosphere-ocean coupled simulations. Calculation performed for subsets of the Baltic Catchment: The entire catchment; sea points; land points north and south of 60 degrees north, respectively. Panels a-d show winter; panels e-h show summer. The lines, with quoted slope and squared correlation coefficient are best fits to all EURO-CORDEX and ENSEMBLES data, but do not include coupled-model results.

345   The relative change in extreme wind speed is shown in Fig. 6 as the relative change of the 10-year return value of daily maximum wind speed for 81 of the Euro-CORDEX simulations considered. Basically nowhere do more than 75% of the models agree on the sign of the pointwise change. It is noteworthy that the interquartile spread is much smaller than in Christensen and Kjellström (2018); this indicates that the models agree that there is no signal, and not just that there are too few models present to overcome natural variability.

350
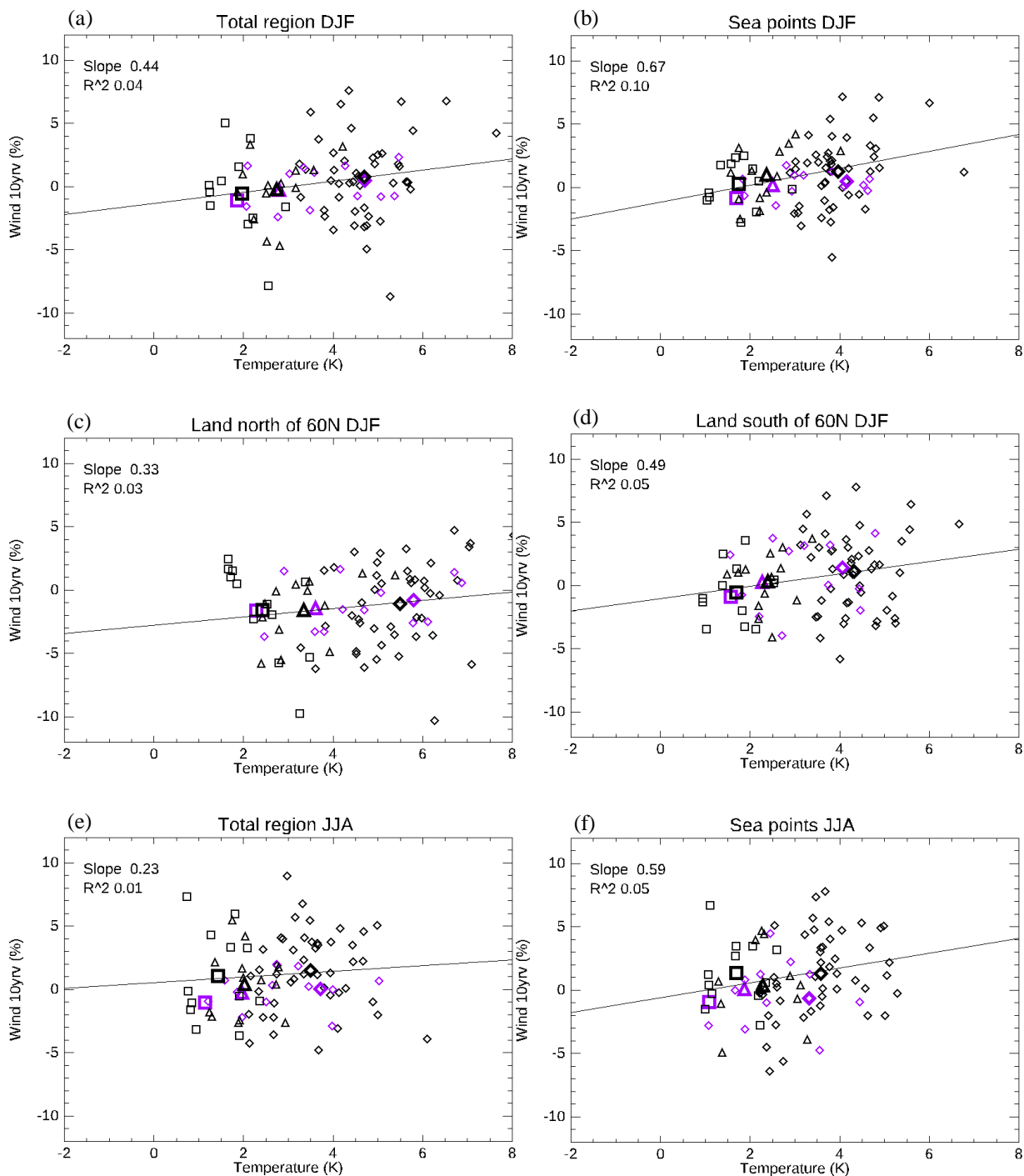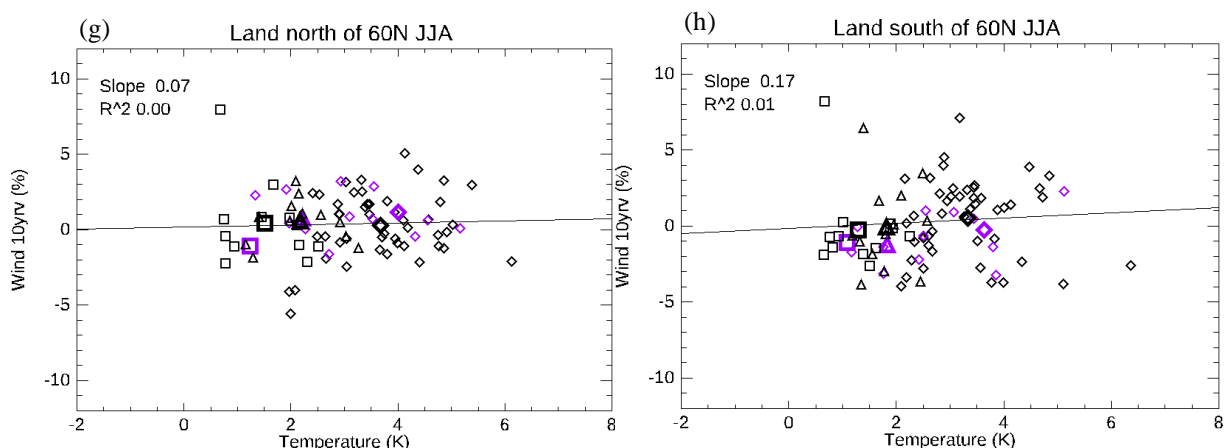
**Figure 6** Relative change 1981-2010 to 2071-2100 of the 10-year return value of 10 m daily maximum wind speed against temperature change for individual models and all scenarios. Scenario means are indicated by larger symbols. Squares: RCP2.6; Triangles: RCP4.5; Diamonds: RCP8.5. Purple colour: The RCA4-NEMO atmosphere-ocean coupled simulations. Calculation performed for subsets of the Baltic Catchment: The entire catchment; sea points; land points north and south of 60 degrees north, respectively. Panels a-d show winter; panels e-h show summer. The lines, with quoted slope and squared correlation coefficient are best fits to all EURO-CORDEX data.

### 3.5 Solar irradiation

In Fig. 7 we study the change in incoming solar radiation in the ensemble, where the pointwise two quartiles and the median are shown. In winter, most of the area shows a considerable relative reduction of the order of 10%. This is attributed to the more extensive cloud cover (not shown) in most models for the future. It should be noted (Bartók et al., 2017) that global and regional models frequently disagree considerably about the change in incoming radiation in a changing climate, with global models having a more positive trend; this discrepancy is connected to different projections of cloud cover, with GCMs frequently projecting a decrease, while RCMs frequently shows no significant change. Also different treatment of aerosols in GCMs and RCMs play a role as many of the RCMs do not include time-varying anthropogenic aerosols leading to weaker future warming compared to GCMs (Boé et al., 2020).
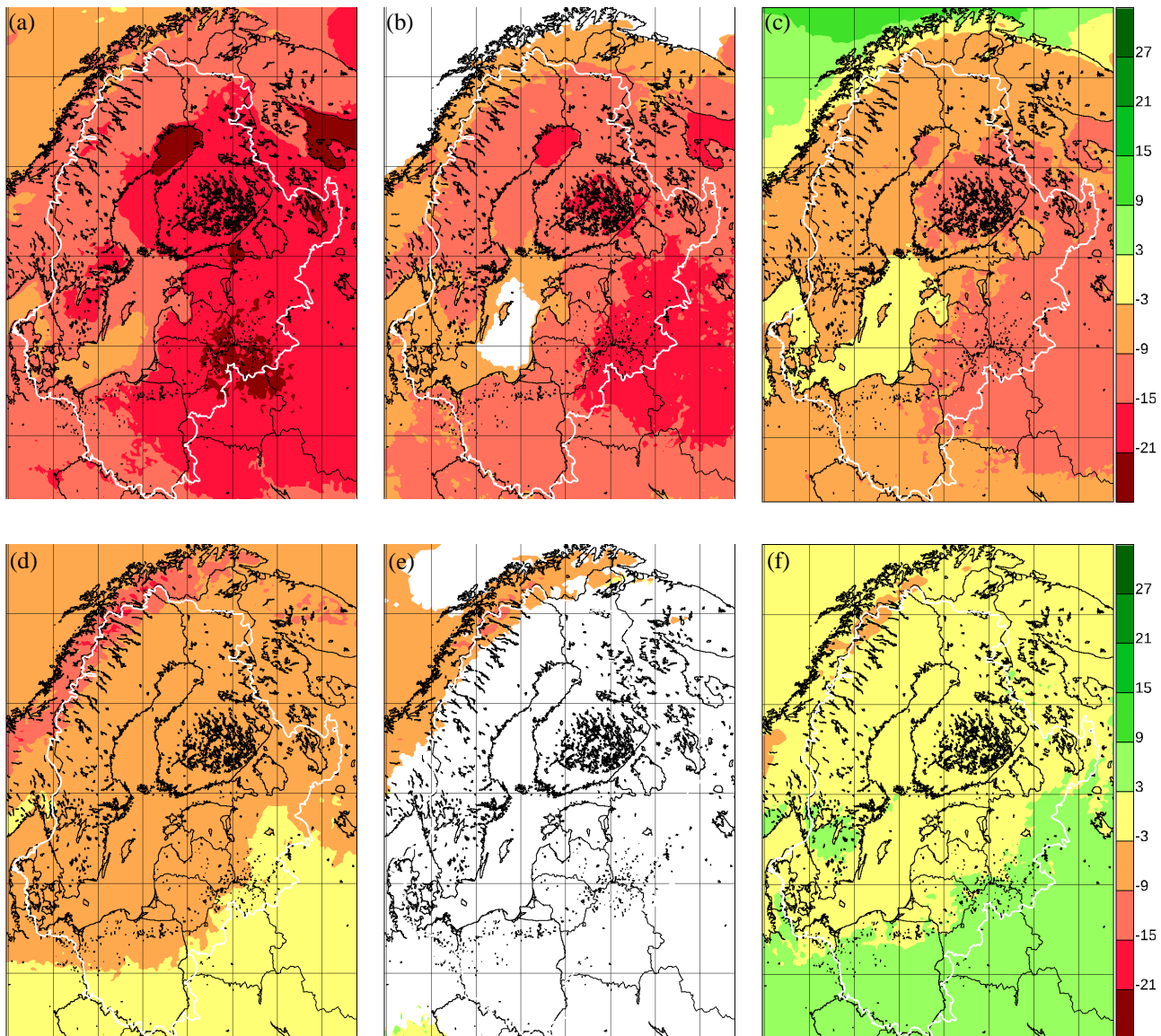
**Figure 7**. Average incoming surface solar radiation relative change between 1981-2010 and 2071-2100 for 70 simulations from Euro-CORDEX according to the RCP8.5 scenario. Panels a-c: Winter; panels d-f: Summer. Panels a,d: lowest quartile; panels b,e: median value; panels c,f: higher quartile. For the medians, only points where 75% of models agree on the sign are shown. The Baltic Sea catchment is indicated in white.

### 3.6 Snow and sea ice

Future snow cover is expected to decrease with climate warming, both because more precipitation is projected to fall as rain, and becausesnow melt accelerates. Simultaneously, there is an increase in winter precipitation in Scandinavia, which may partly compensate for these effects.

Räisänen and Eklund (2011) analysed data from RCM simulations from the ENSEMBLES project. The study found a decrease of snow volume across all of Europe in the future with the only exception that the Scandinavian mountain areas may experience a slight and statistically insignificant increase. An increase in the latter region was also proposed by Schuler et al. (2006) in a detailed study for Norway based on two RCM simulations with different GCM drivers. The study concluded that the maximum amount of snow in extreme years could be greater than in extreme years of the recent past in spite of decreasing average snow amount.

Winter snow cover is one of the most drastically changed climatological quantities (Fig. 8). There is agreement between models about a reduction of average winter-time snow amount of around 50% on average for land grid points north of 60°N for the RCP8.5 scenario, and almost 80% reduction for land grid points south of this latitude. Northern grid points probably have a lower reduction due to a significant amount of mountain grid points, where the warming temperature does not reach the freezing point as frequently as in lower-lying regions even if the frequency is increasing in a warmer climate (Nilsen et al. 2021). The reduction in snow amount is slightly larger than in BACC II (BACC II Author Team, 2015), consistent with the fact that the RCP8.5 scenario on average projects larger warming than the SRES A1B scenario used in BACC II.

It is only in high-altitude parts of central and northern Scandinavia that changes are limited with relatively large amounts of snow also in the future. At high altitude, the increase of winter precipitation may be compensating for the increase in melting with higher temperature. Also the fact that increasing temperatures may not reach the melting point is significant.

Sea ice cover is not a product of the RCM, but rather an input originating from the driving GCM. We will show the changes in interpolated sea ice field for the RCP8.5 scenario in Fig. 9, as these changes are large, and are decisive for the change in climate between the periods. In order to compare to a more consistent description of sea ice we also show in Fig. 10 the corresponding figures for the 8-member RCA4-NEMO coupled regional simulations. The main difference is that the present-day simulations with the coupled model have some extent of coastal sea ice, which is disappearing in the future.
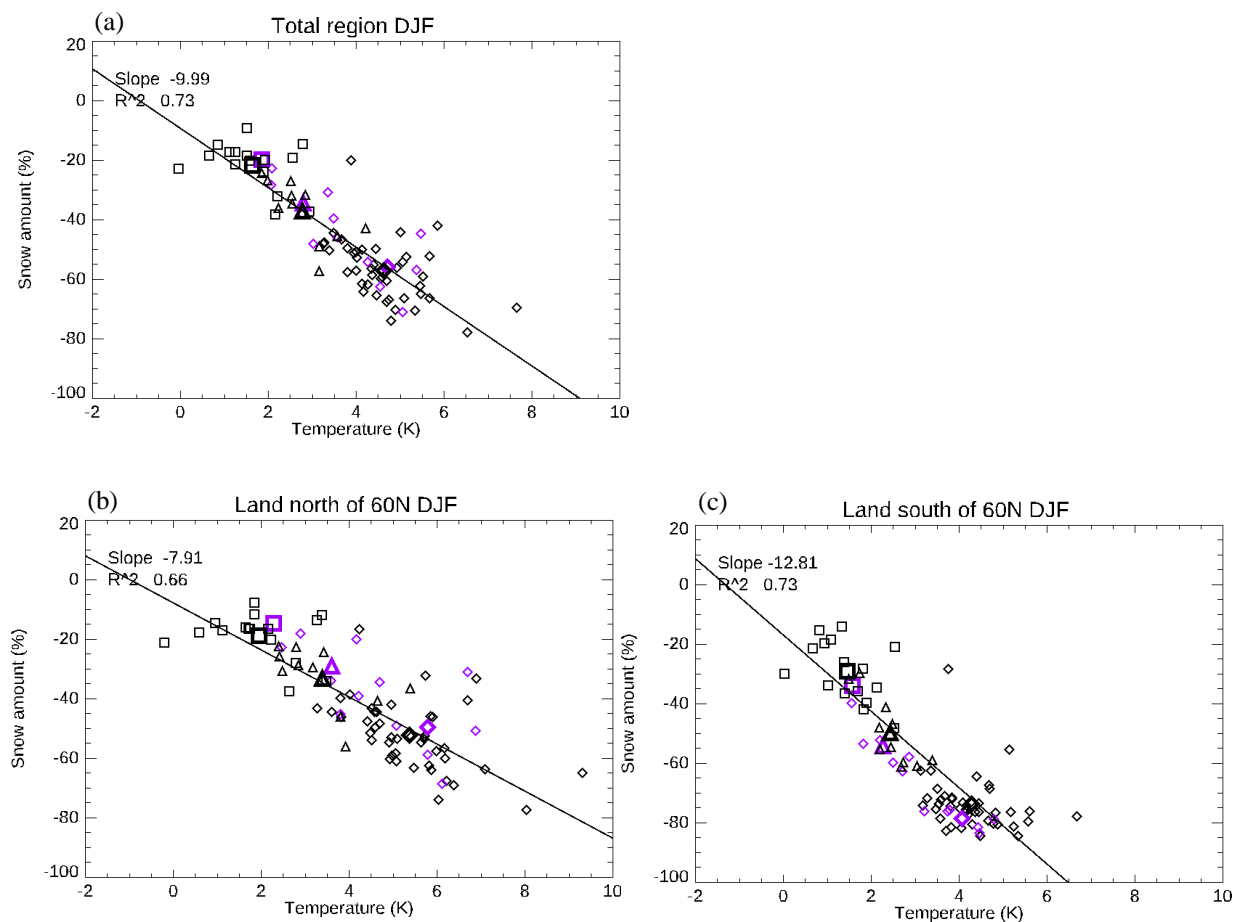
**Figure 8** Relative change 1981-2010 to 2071-2100 of average winter (DJF) snow amount (kg/m$^2$) against temperature change for 84 individual model simulations from all scenarios. Scenario means are indicated by larger symbols. Squares: RCP2.6; Triangles: RCP4.5; Diamonds: RCP8.5. Purple colour: The RCA4-NEMO atmosphere-ocean coupled simulations. Calculation performed for subsets of land points in the Baltic Catchment: The entire catchment; land points north and south of 60 degrees north, respectively. The lines, with quoted slope and squared correlation coefficient are best fits to all EURO-CORDEX data, but do not include coupled-model results.

410
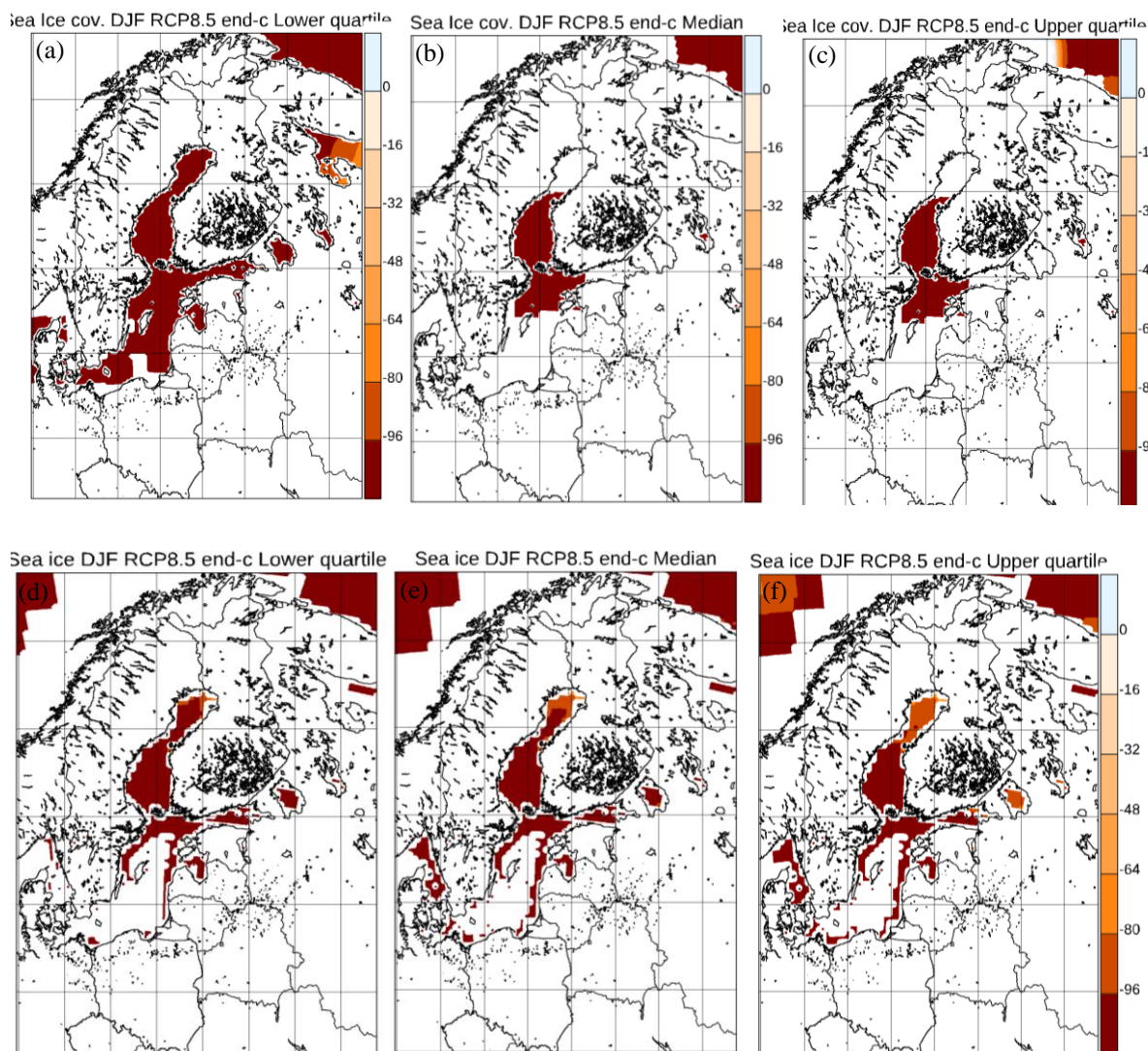
**Figure 9**. Panels a-c: Average winter sea ice cover relative change between 1981-2010 and 2071-2100 for the simulations from Euro-CORDEX according to the RCP8.5 scenario driven by the GCMs where RCA4-NEMO simulations exist. These values have been interpolated before the RCM simulations from the driving coupled GCM; note that several simulations have sea ice in the Baltic Sea in the present-day period, but not in the Bay of Bothnia. For comparison, in panels d-f we also show the corresponding fields from the corresponding five coupled RCA4-NEMO simulations where sea ice cover is calculated inside the regional model. Left column: lowest quartile; mid column: median value; right column: higher quartile. For the medians, only points where 75% of models agree on the sign are shown.

## 4   Effects of model coupling

Here, we take a more detailed look at the five driving GCMs, which have been downscaled both by the standalone atmosphere EURO-CORDEX ensemble and by the 24 km RCA4-NEMO coupled model version.

For near-surface air temperature (Fig. 10) the large-scale anomaly pattern is fairly coherent in the two ensembles but differences are found over the northern Baltic Sea where the coupled model shows a systematically stronger winter warming than the uncoupled model. By contrast, during summer the coupled model shows a weaker warming over the entire Baltic Sea than the RCA standalone.

Due to its higher effective heat capacity, the Baltic Sea acts as a thermal buffer, which dampens the seasonal amplitude compared to the surrounding land areas. As a result, the Baltic Sea is warmer than the overlying atmosphere during winter and releases heat to the atmosphere. Hence, in regions not covered by sea ice, the SST significantly influences the sea to air heat flux. Consequently, in the uncoupled model the prescribed SSTs from the driving AOGCM serve as a restoring term for the air temperature. By contrast, in the coupled model SSTs are simultaneously modelled by the ocean model and so the air to sea heat transfer acts to cool SSTs until a new equilibrium would be reached. Despite these different dynamics in thermal coupling, over the southern Baltic Sea the solution of the two models is quite similar compared to the northern Baltic (Fig. 10). This is probably due to the fact that air temperature anomalies generated locally over the open sea disperse rapidly in the atmosphere.

In the northern Baltic Sea, the reduction of sea ice has to be considered. In the future climate, areas which today are isolated by sea ice will get more tightly thermally coupled to the water body of the Baltic Sea. As shown by Gröger et al. (2015, 2020a, 2021b) the ocean to atmosphere heat transfer is largely affected by small-scale vertical mixing in the layered ocean because wind induced mixing transports warm waters from deeper water layers to the surface. These small scale processes are most likely not well represented in the prescribed SST from the driving global ocean GCM. Furthermore, changes in the mean and turbulent wind stress due to local climate change in RCA have no impact on wind induced mixing in the ocean in RCA standalone. This further influences the local sea ice cover and thus may explain the stronger warming over the northern Baltic Sea in the coupled model compared to the uncoupled version of RCA. In the atmosphere, a stronger thermal coupling to the water body changes not only near-surface temperatures but also modifies atmospheric stability and thereby mixing of heat, moisture and momentum with potential impacts on temperature, precipitation and winds.

During summer when the Baltic Sea takes up heat from the atmosphere, the air - sea heat exchange is greatly influenced by the water bodies' thermocline layer which is in the order between 10 to 30 meter thickness (e.g. Gröger et al., 2019). Thermocline dynamics is likely much more realistically represented when explicitly modelled by a coupled high resolution ocean RCM rather than reflected in prescribed SST taken from a global GCM of coarse resolution. Winter precipitation (Fig. 11) displays a fairly coherent change signal for the coupled and uncoupled RCA projections. The only noteworthy exception

is the topographically elevated area along the Norwegian coast which in RCA standalone exhibits slight increases of up to 5% for the 25th for the lower quartile. In contrast to this, for the RCA coupled version the change is in the opposite direction and shows locally up to 15 % less precipitation. However, since in this area precipitation is strongly affected by orography the differences are likely related to the differences in resolution (12 km vs. 24 km). During summer, the coupled model 455 exhibits a more intense decrease of lower quantile precipitation in the south and the increase in the north is less well pronounced compared to RCA standalone. This pattern translates into less coherent signals for the median precipitation which points to a larger spread among ensemble members far into North Scandinavia (Fig. 11, middle).

A prominent feature of winter wind speed changes is the strong decreases along the Norwegian coast seen in all three quartiles in the coupled RCA model. This is less pronounced in the uncoupled runs. However, in those regions with steep 460 topographic gradients the difference can be likely attributed to the differing grid resolutions though coupling effects cannot be excluded. For most other land regions winds are slightly weakened in the lower and slightly strengthened in the higher quartile and a consequently high uncertainty is seen for median winds. This is probably an effect of the different resolution of the two ensembles.

A noteworthy difference between coupled and uncoupled simulations during winter is the stronger intensification for all 465 three quartile wind speeds over the northern Baltic Sea region, especially over the Bay of Bothnia. This points to local coupled feedback processes probably related to the vanishing sea ice, higher sea-surface temperatures and altered atmospheric static stability. A larger decrease in sea-ice and a stronger coupling between the atmosphere and the water body leads to a stronger heat flux to the atmosphere and thereby reduced vertical stability. This, in turn, leads to a more efficient downward mixing of momentum in the lower atmosphere and consequently higher wind speed close to the sea surface.

470 Summer changes in wind speed are highly coherent between the coupled and uncoupled simulations. Moderate differences, however, occur over the Baltic Sea where the lower quartile decrease is more pronounced in the coupled model. The higher quartile shows wide areas of wind speed increases in the uncoupled version while in the coupled model changes are very low (< 2m/s). The latter differences might be explained by the smaller SST increase in the coupled compared to the uncoupled simulations indicating less destabilization of the near surface PBL. This difference in stratification would act to 475 reduce wind speed changes, contrary to the winter situation.

The changes between future and present climate conditions in solar irradiation (Figs. 15 and 16) are closely linked to changes in cloud cover. Both RCA versions simulate a generally less pronounced reduction in solar radiation during winter than the average reduction seen in the entire EURO-CORDEX ensemble (Fig. 7). Strongest reductions are found over the Bothnian Sea where vanishing sea ice exposes open water to the atmosphere formerly isolated by sea ice. In both models, the 480 reduction in solar radiation is more obvious in the lower quartile and median irradiance as the higher quartile generally reflects more low-cloud or even cloud free conditions already during the historical climate. Compared to the coupled

version, the uncoupled RCA reveals a stronger reduction over the Bothnian Bay for days with an irradiance lower than the median while the opposite is found for the higher quartile (Fig. 15).

485 To fully understand the different responses, detailed process analysis including the respective ocean dynamics would be necessary to draw general conclusions. In addition, the here described systematic coupled vs. uncoupled differences may be specific with regard to the employed RCA regional atmosphere model and the coupled NEMO ocean RCM. Also, the atmospheric part of the model, RCA, is run with different resolution in the coupled and uncoupled simulations, which may have an impact on the results. Hence, the here found systematic differences should be tested in coordinated experiments including also with other coupled and uncoupled systems.

490 Finally, we note that the coupling area comprising the North Sea and Baltic Sea only is relatively small compared to entire Euro-Cordex domain and there is indication that coupling effects may be more important if other seas, such as the Mediterranean or the NE Atlantic, are included (e.g. Kelemen et al., 2019, Primo et al., 2019; Akhtar et al., 2019; Gröger et al., 2021b). The potential of different coupling techniques to influence the response of atmospheric large-scale circulation to climate change has been found to be most important during the winter season.

495

T DJF RCP8.5 end-c Lower quartile     T DJF RCP8.5 end-c Median     T DJF RCP8.5 end-c Upper quartile

T DJF RCP8.5 end-c Lower quartile     T DJF RCP8.5 end-c Median     T DJF RCP8.5 end-c Upper quartile
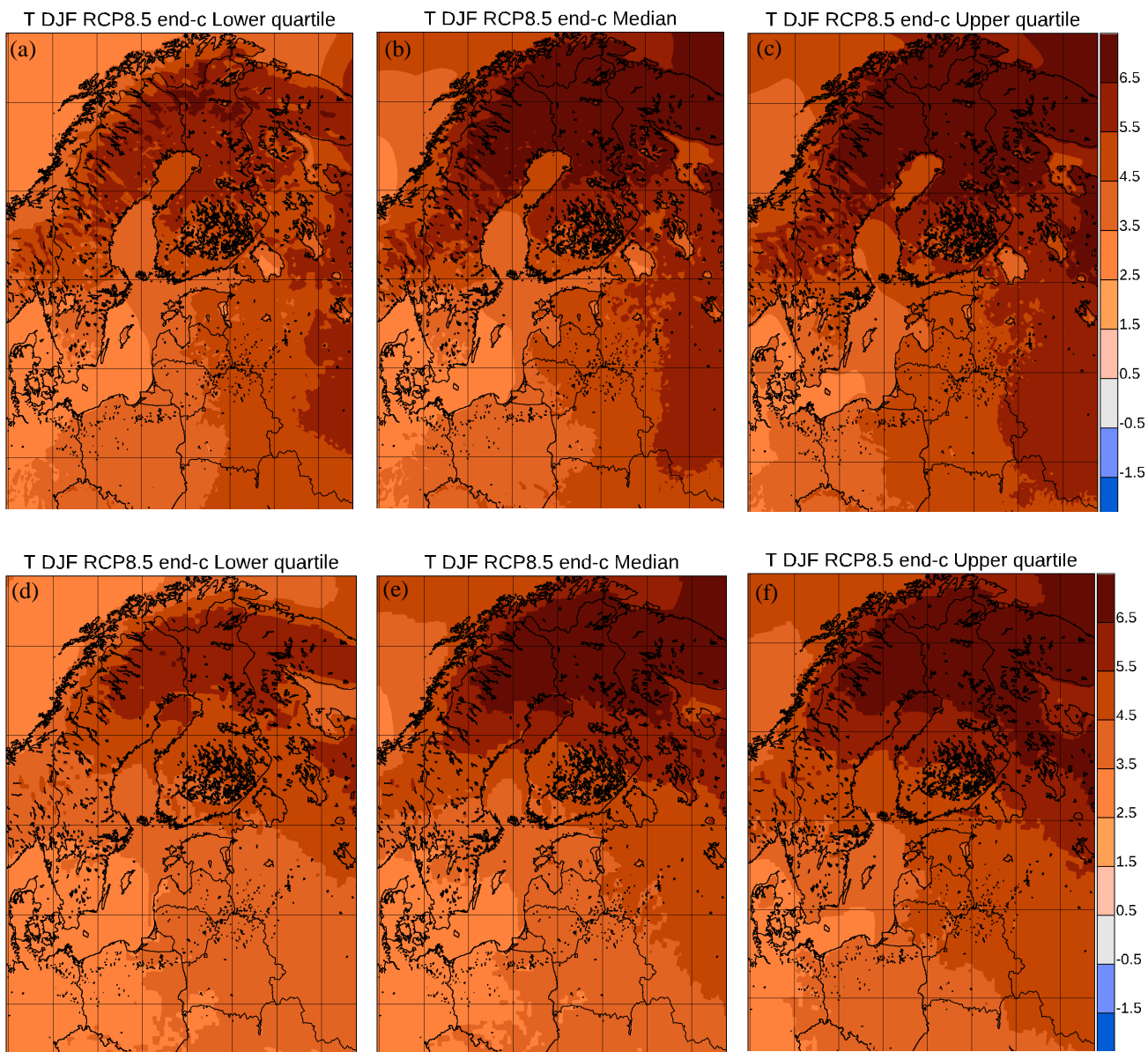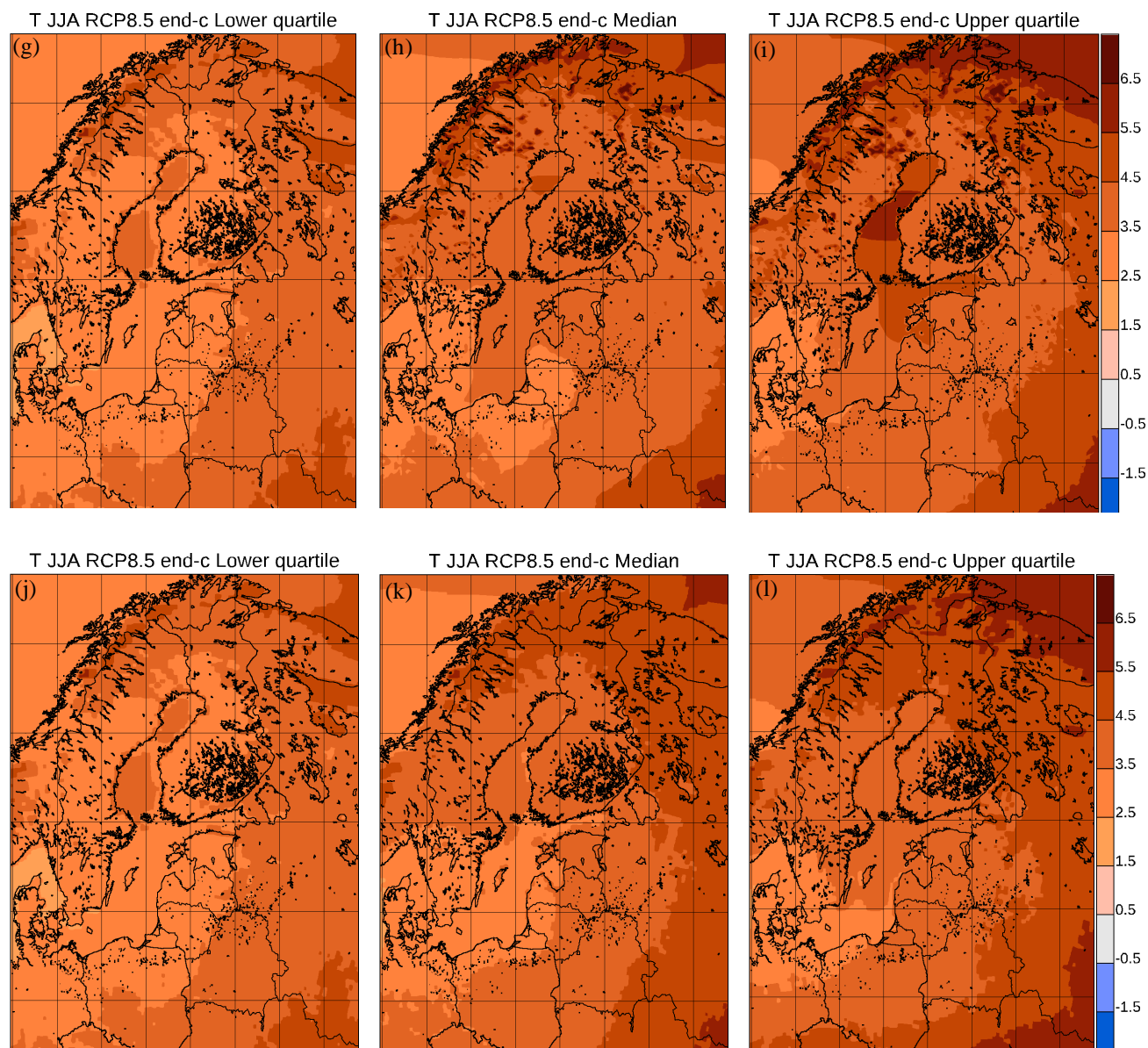
**Figure 10.** Temperature change between 1981-2010 and 2071-2100 for 5 atmosphere-only RCA4 simulations from Euro-CORDEX according to the RCP8.5 scenario and for the coupled single-model RCA4-NEMO ensemble with the same driving GCMs. Left column (panels a,d,g,j): lowest quartile; mid column (panels b,e,h,k): median value; right column (panels c,f,i,l): higher quartile. The mid column depicting pointwise median values is only coloured when 75% of simulations agree on the sign of the change.

Precip DJF RCP8.5 end-c Lower quartile    Precip DJF RCP8.5 end-c Median    Precip DJF RCP8.5 end-c Upper quartile

(a)                                       (b)                                (c)

recip DJF RCP8.5 end-c Lower quartile     Precip DJF RCP8.5 end-c Median    Precip DJF RCP8.5 end-c Upper quartile

(d)                                       (e)                                (f)
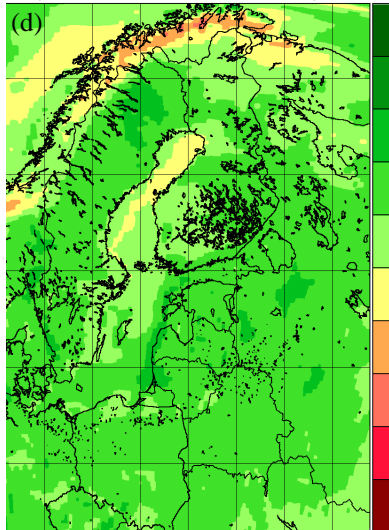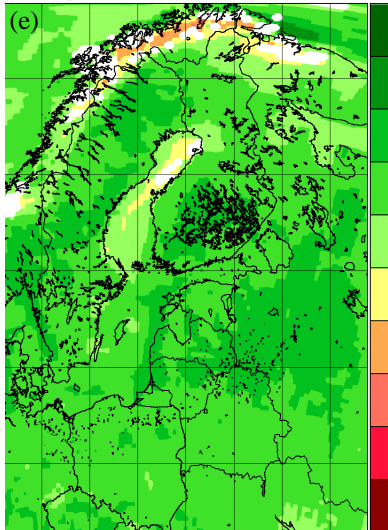
**Figure 11**. Precipitation relative change (%) between 1981-2010 and 2071-2100 for 5 atmosphere-only RCA4 simulations from Euro-CORDEX according to the RCP8.5 scenario and for the coupled single-model RCA4-NEMO ensemble with the same driving GCMs. Left column (panels a,d,g,j): lowest quartile; mid column (panels b,e,h,k): median value; right column (panels c,f,i,l): higher quartile. The mid column depicting pointwise median values is only coloured when 75% of simulations agree on the sign of the change.

510
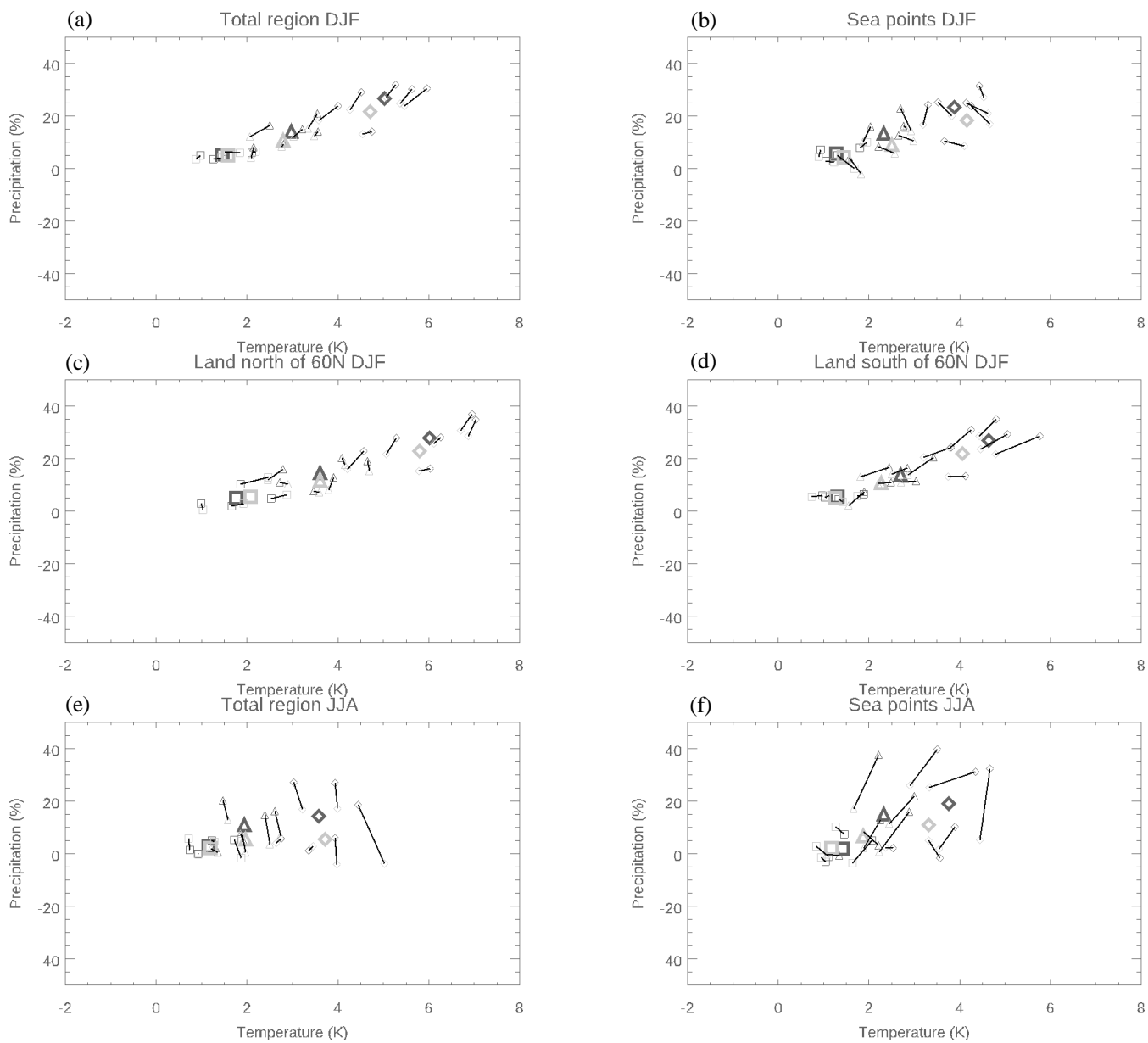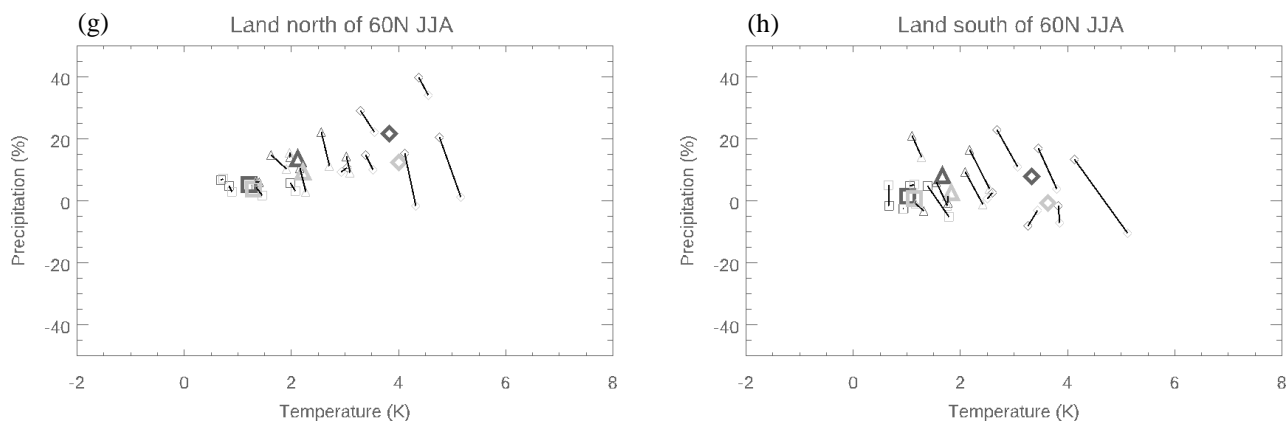
**Figure 12** Relative change 1981-2010 to 2071-2100 of precipitation against temperature change for the models where both coupled and uncoupled higher-resolution simulations exist. Model pairs are connected with lines. Scenario means are indicated by larger symbols. Squares: RCP2.6; Triangles: RCP4.5; Diamonds: RCP8.5. Pale colours: The RCA4-NEMO atmosphere-ocean coupled simulations. Calculation performed for subsets of the Baltic Catchment: The entire catchment; sea points; land points north and south of 60 degrees north, respectively. First 4 panels show winter; the following 4 panels show summer.
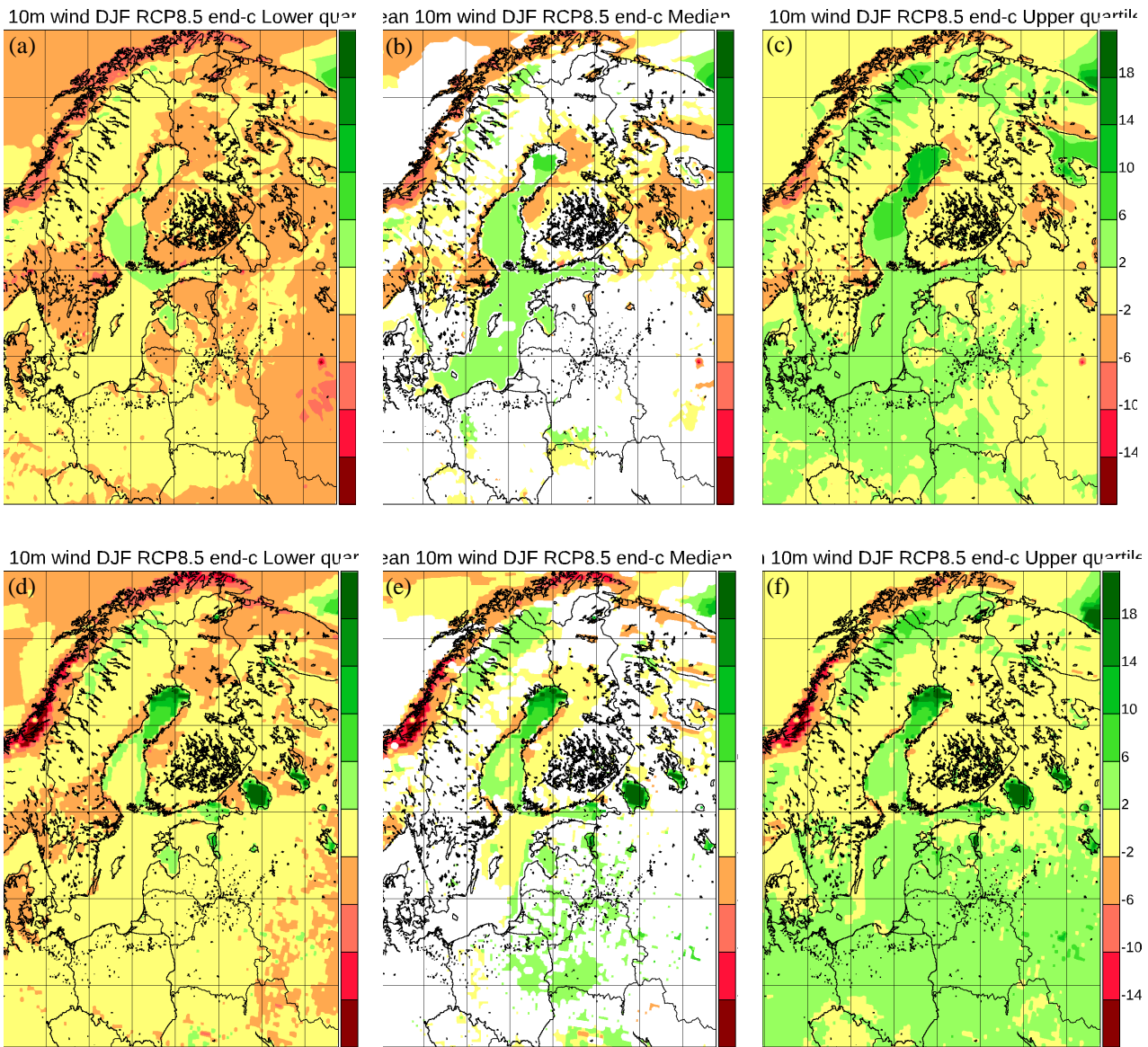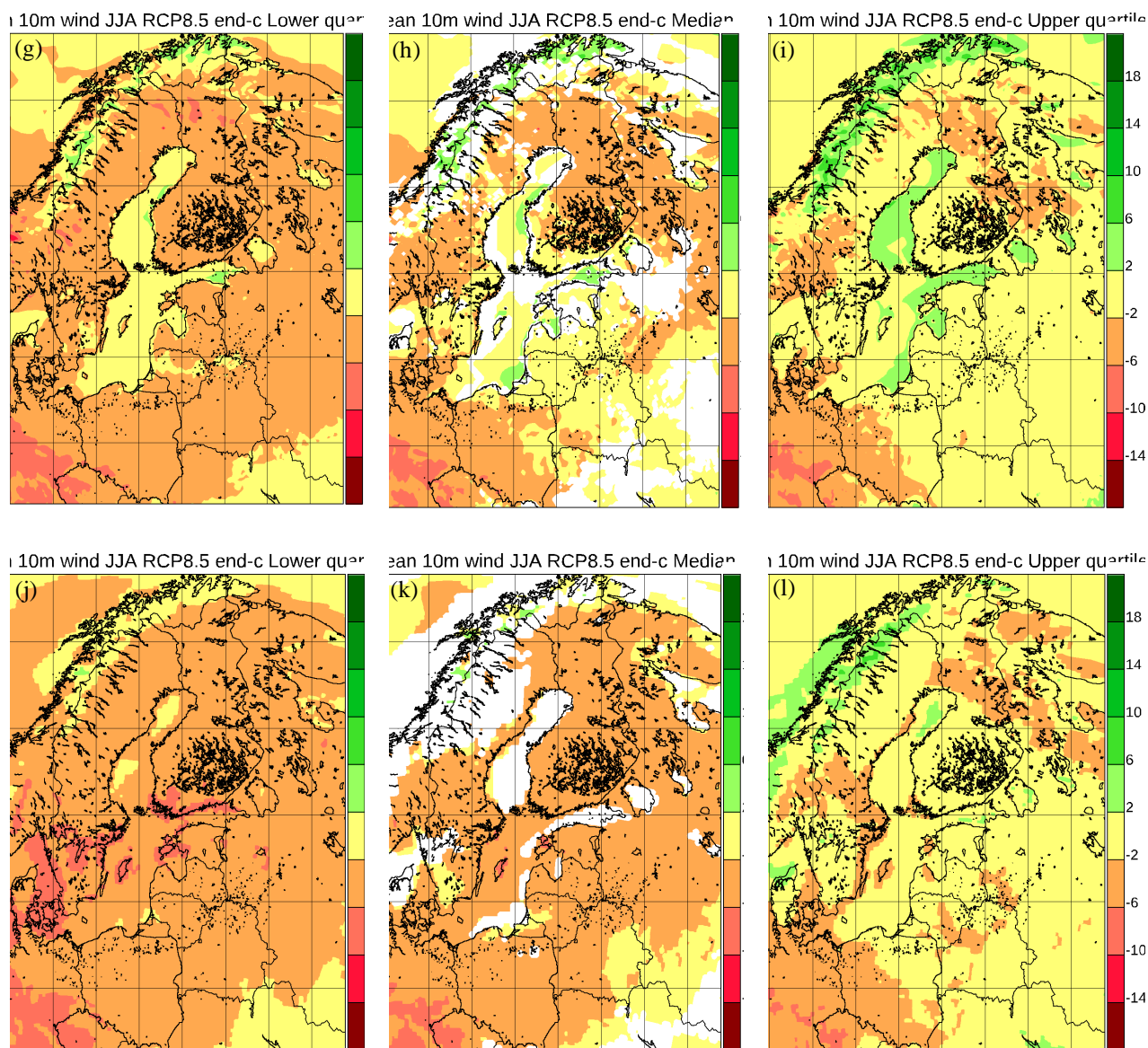
**Figure 13**. Average wind speed relative change (%) between 1981-2010 and 2071-2100 for 5 atmosphere-only RCA4 simulations from Euro-CORDEX according to the RCP8.5 scenario and for the coupled single-model RCA4-NEMO ensemble with the same driving GCMs. By row: Euro-CORDEX winter; RCA4-NEMO winter; Euro-CORDEX summer; RCA4-NEMO summer. Left column (panels a,d,g,j): lowest quartile; mid column (panels b,e,h,k): median value; right column (panels c,f,i,l): higher quartile. The mid column depicting pointwise median values is only coloured when 75% of simulations agree on the sign of the change.
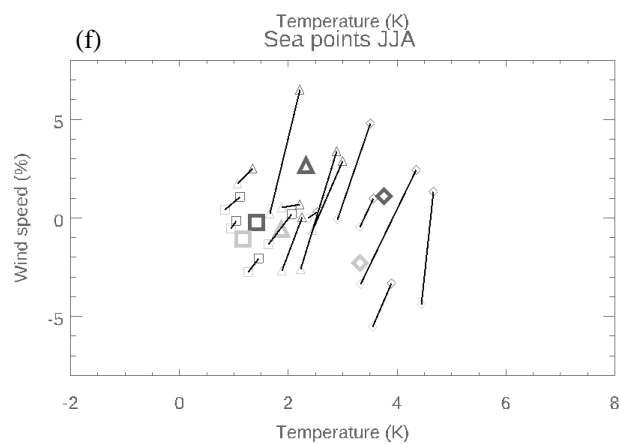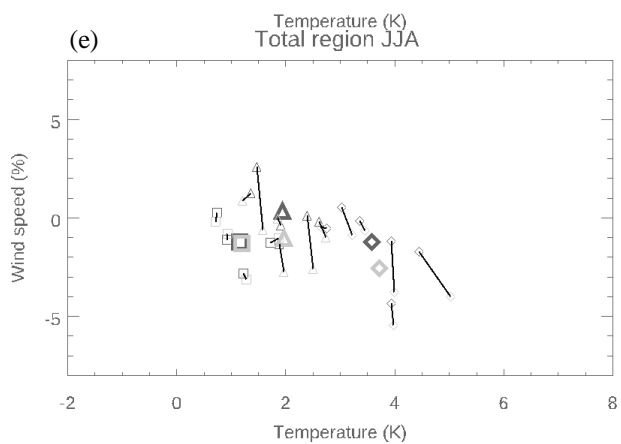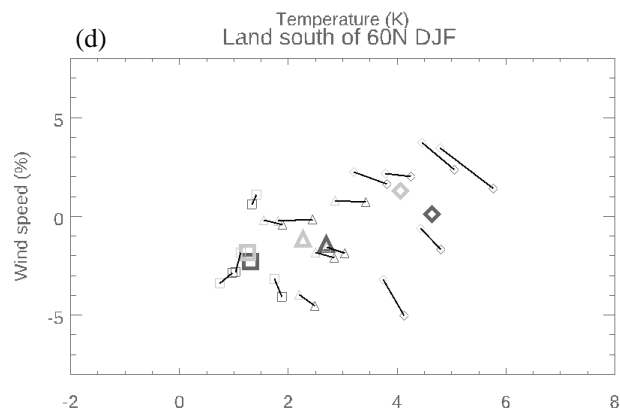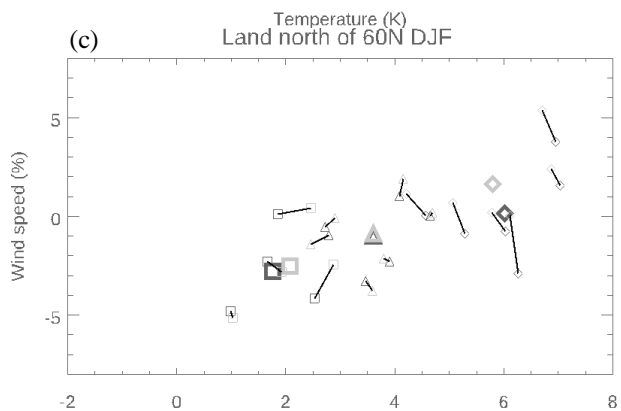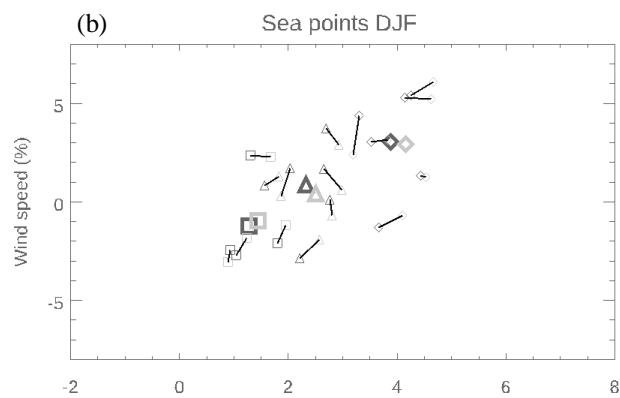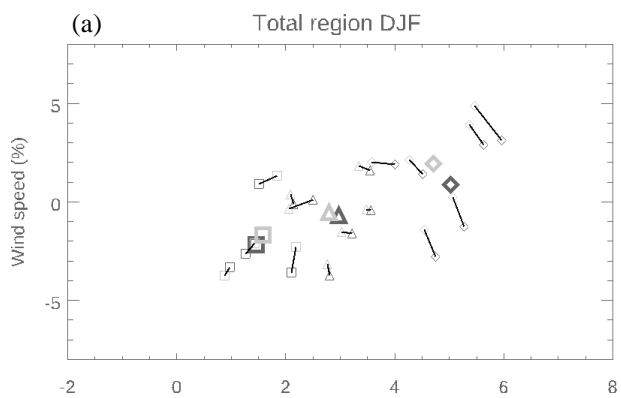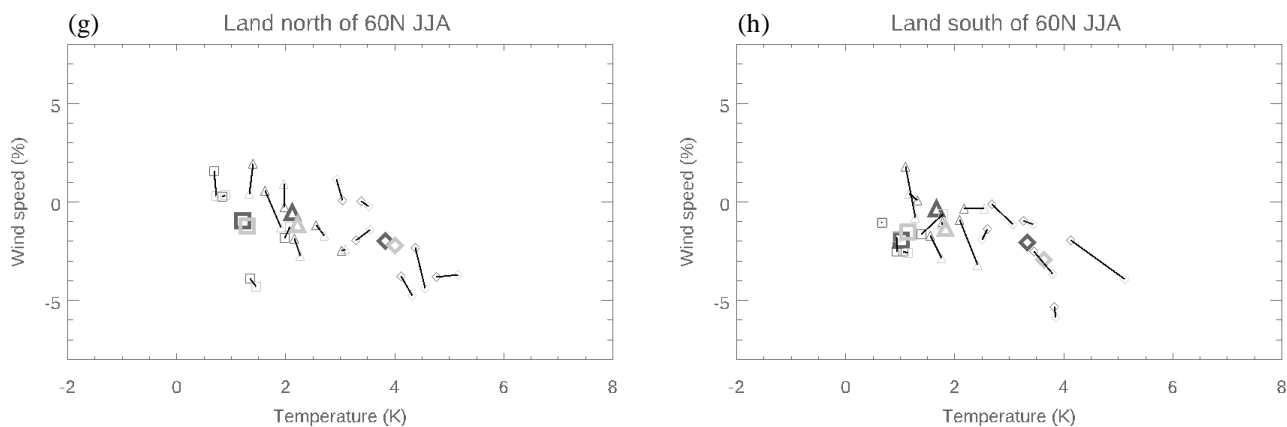
**Figure 14** Relative change 1981-2010 to 2071-2100 of the average 10m wind speed against temperature change for the models where both coupled and uncoupled higher-resolution simulations exist. Model pairs are connected with lines. Scenario means are indicated by larger symbols. Squares: RCP2.6; Triangles: RCP4.5; Diamonds: RCP8.5. Pale colours: The RCA4-NEMO atmosphere-ocean coupled simulations. Calculation performed for subsets of the Baltic Catchment: The entire catchment; sea points; land points north and south of 60 degrees north, respectively. Panels a-d show winter; panels e-h show summer.

ming SW DJF RCP8.5 end-c Lower qua'coming SW DJF RCP8.5 end-c Median  coming SW DJF RCP8.5 end-c Upper quartile

ming SW DJF RCP8.5 end-c Lower qua'coming SW DJF RCP8.5 end-c Median coming SW DJF RCP8.5 end-c Upper quartile

**Figure 15**. Average incoming solar radiation relative change (%) between 1981-2010 and 2071-2100 for 5 atmosphere-only RCA4 simulations from Euro-CORDEX according to the RCP8.5 scenario and for the coupled single-model RCA4-NEMO ensemble with the same driving GCMs. Panels a-c: Euro-CORDEX winter; panels d-f: RCA4-NEMO winter; panels g-i: Euro-CORDEX summer; panels j-l: RCA4-NEMO summer. Left column (panels a,d,g,j): lowest quartile; mid column (panels b,e,h,k): median value; right column (panels c,f,i,l): higher quartile. The mid column depicting pointwise median values is only coloured when 75% of simulations agree on the sign of the change.
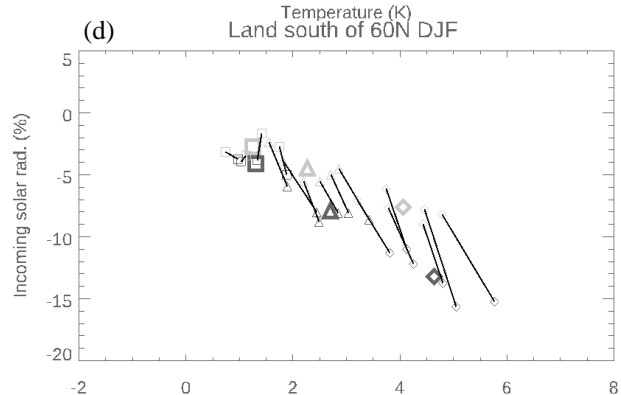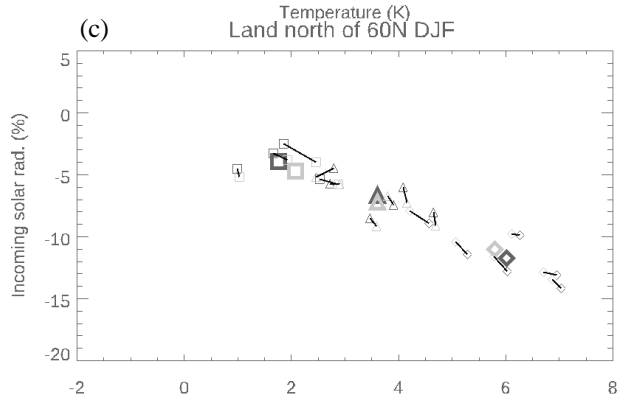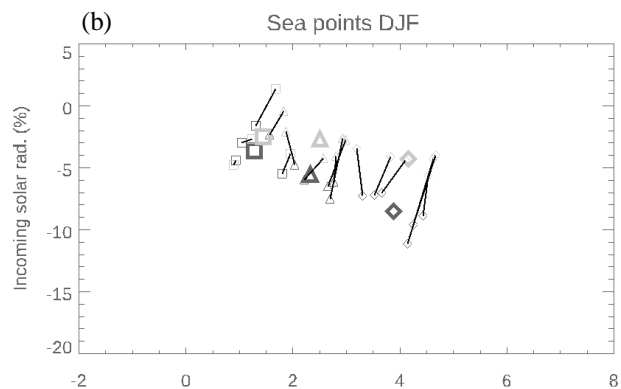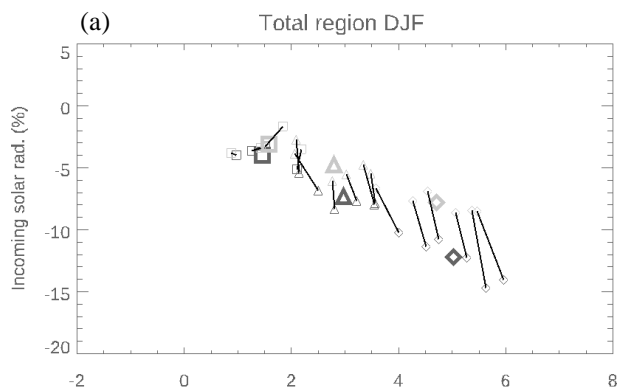
545
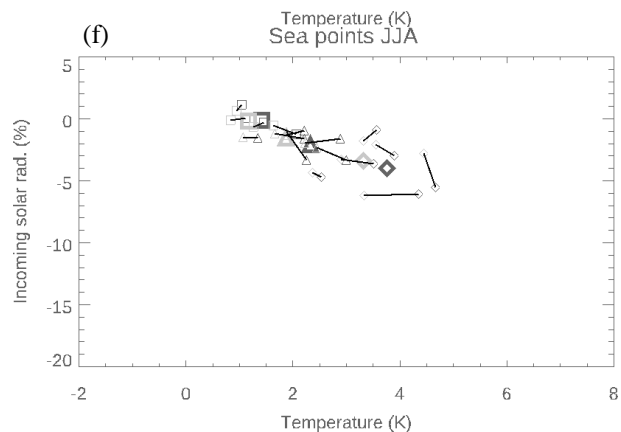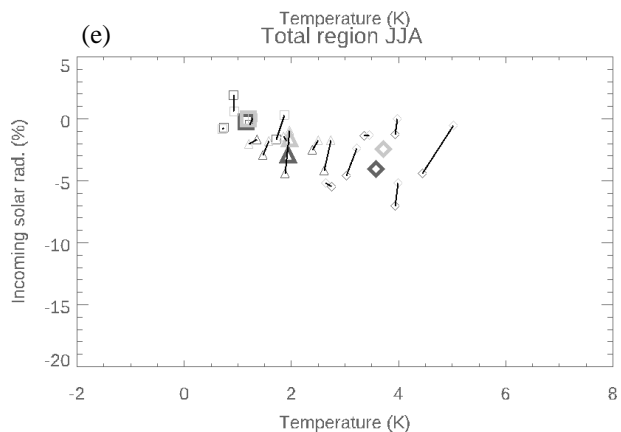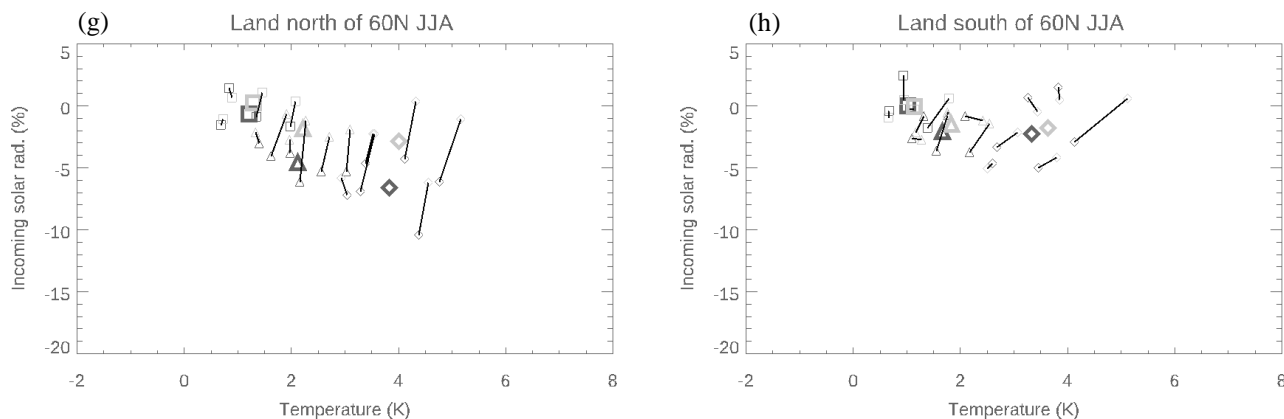
**Figure 16** Relative change 1981-2010 to 2071-2100 of the incoming solar radiation against temperature change for the models where both coupled and uncoupled higher-resolution simulations exist. Model pairs are connected with lines.
550   Scenario means are indicated by larger symbols. Squares: RCP2.6; Triangles: RCP4.5; Diamonds: RCP8.5. Pale colours: The RCA4-NEMO atmosphere-ocean coupled simulations. Calculation performed for subsets of the Baltic Catchment: The entire catchment; sea points; land points north and south of 60 degrees north, respectively. Panels a-d show winter; panels e-h show summer.

## 5   Conclusions

555   Since the previous BACC reports from 2008 and 2015, a very large amount of high-resolution regional climate model simulations have been performed over Europe, mostly downscaling global simulations from CMIP5. We have presented ensemble model results here, and we have compared the climate change results to those of BACC II (BACC II Author Team, 2015). The regional climate model simulations of BACC II were using a different emission scenario (SRES A1B) and a different set of GCMs than the currently used RCP scenarios from CMIP5. We have therefore chosen to compare the results 560   as a function of local temperature change.

The results, illustrated for seasonal-mean precipitation (Fig. 3) and wind speed (Fig. 5), do not indicate any significant change in the relation of these fields to local temperature change since BACC II. However, the much larger ensemble of scenario simulations allows for a more reliable assessment of future climate change compared to earlier studies. This is illustrated in the figures showing how the increase in the number of simulations, particularly the many more global models 565   considered, has given much more credibility to estimates of robustness and uncertainty. This is the case both for local climate sensitivity, as illustrated by the different temperature change values for downscaling of each individual emission scenario, and for the inter-variable relations as illustrated with the general scatter of the points. Also, the addition of several emission scenarios enables a better foundation for estimating effects of e.g. emission mitigation.

The local temperature increases of current RCP8.5 simulations are close to the A1B results of BACC II, in spite of the stronger average global warming in the underlying RCP8.5 GCM ensemble compared to that in the A1B GCM ensemble. The difference in global mean by the end of the century is 0.7K, i.e. about 25%. The regional sensitivity to global climate change is therefore somewhat smaller than it was in BACC II.

The expected anthropogenic climate change for the Baltic Sea area is corroborated by the present results: Temperature will increase, in step with global warming, and with a north-south gradient. In the northern part of the area in winter, the warming approaches twice the average global warming.

Precipitation increases over the entire area in winter, somewhat less in summer in the northern part of the domain, and it does not change significantly in summer in the southern part. Extreme precipitation, here the 10-year return value, increases systematically, particularly in summer, in the entire domain, with some simulations showing more than 50% increase.

The large ensemble of simulations does not indicate significant change in wind speed. However, individual model simulations show strong differences. Consequently, there is a strong uncertainty related to future wind speed change in the area.

Solar irradiation at the surface is not projected to change in summer, but the RCM simulations show some decrease in winter connected to more extensive cloud cover in the future. There is, however, a large uncertainty related to this, since many GCMs show the opposite sign of the trend.

Snow cover, measured as the average amount of snow on the ground in winter (DJF), is reduced drastically, particularly in the south of the Baltic Sea Catchment, where the relative decrease is close to 80%.

With respect to coupled vs. uncoupled models, we find a stronger warming in the coupled model during winter which is most pronounced in areas that today are seasonally affected by sea ice. During summer the coupled model shows weaker warming compared to the uncoupled model. The comparison between coupled and uncoupled versions of a small subset of projections with the RCA4 and RCA4-NEMO models generally confirms results of Gröger et al. (2021b) who found coupling effects for most climate indices changes most important over the interactively coupled flat open sea area. Notable differences outside the coupled region occur over regions of topographically elevated terrain suggesting further significant uncertainty due to model resolution.

**Declarations**

595 **Funding**

This study has been partly funded by the Copernicus Climate Change Service. ECMWF implements this Service on behalf of the European Commission. Also, it has been partly funded by the Danish state through the Danish National Centre for Climate Research (NCKF).

**Availability of data and material**

600 All data used in this publication are publicly available through the ESGF network, e.g., http://esgf-data.dkrz.de.

**Code availability**

All data manipulations in this study are straightforward and described in the manuscript

**Acknowledgements**

The research presented in this study is part of the Baltic Earth Assessment Reports project of the Baltic Earth program (Earth
605 System Science of the Baltic Sea Region, https://www.baltic.earth ). The authors would like to thank the Euro-CORDEX network and WCRP CORDEX for ensuring availability of CORDEX data.

It is with great sadness that we received the news that our co-author Christian Dieterich passed away during the review of this manuscript.

**References**

610 Akhtar, N., Krug, A., Brauch, J., Arsouze, T., Dieterich, C., Ahrens, B.: European Marginal Seas in a regional atmosphere-ocean coupled model and their impact on Vb-cyclones and associated precipitation, Clim Dynam, 2019, 1-33, https://doi.org/10.1007/s00382-019-04906-x, 2019

BACC Author Team (2008) Assessment of Climate Change for the Baltic Sea Basin. Regional Climate Studies, Springer Verlag, Berlin, Heidelberg

615 BACC II Author Team (2015) Second Assessment of Climate Change for the Baltic Sea Basin. Regional Climate Studies, Springer Verlag, Berlin, Heidelberg

Ban, N., Schmidli,J., and Schär, C.: Heavy precipitation in a changing climate: Does short-term summer precipitation increase faster?, Geophys. Res. Lett., 42, 1165–1172, doi:10.1002/2014GL062588, 2015.

Bartók, B., Wild, M., Folini, D.*et al.*:Projected changes in surface solar radiation in CMIP5 global climate models and in
620 EURO-CORDEX regional climate models for Europe. *Clim Dyn* **49**, 2665–2683. https://doi.org/10.1007/s00382-016-3471-2, 2017

Boé J., Somot S., Corre L., and Nabat .: Large discrepancies in summer climate change over Europe as projected by global and regional climate models: causes and consequences. Clim Dyn 54, 2981–3002. https://doi.org/10.1007/s00382-020-05153-1 2020.

625 Buser, C. M., Künsch, H. R., and Schär, C.: Bayesian multi-model projections of climate: generalization and application to ENSEMBLES results. Clim Res 4:227-241 2010.

Christensen, J. H., Larsen, M. A. D., Christensen, O. B., Drews, M., and Stendel, M.: Robustness of European climate projections from dynamical downscaling, Clim. Dyn., 2019, https://doi.org/10.1007/s00382-019-04831-z, 2019.

Christensen, J. H., and Christensen O. B.: Severe summertime flooding in Europe. Nature 421:805-806, 2003.

630 Christensen, J. H., and Christensen, O. B.: A summary of the PRUDENCE model projections of changes in European climate by the end of the century. Climatic Change 81:7-30, 2007.

Christensen JH, Hewitson B, Busuioc A, Chen A, Gao X, Held I, Jones R, Kolli RK, Kwon WT, Laprise R, Magaña Rueda V, Mearns L, Menéndez CG, Räisänen J, Rinke A, Sarr A,Whetton P (2007) Regional Climate Projections. In: Solomon S, Qin D, Manning M, Chen Z, Marquis M, Averyt KB, Tignor M, Miller HL (eds), Climate Change 2007: The Physical
635 Science Basis. Contribution of Working Group I to the Fourth Assessment Report of the Intergovernmental Panel on Climate Change. Cambridge University Press, Cambridge, UK

Christensen J. H., Kjellström E., Giorgi, F., Lenderink, G., and Rummukainen, M.: Weight assignment in regional climate models. Clim Res 44:179-194 2010.

Christensen O. B., Kjellström E., Zorita E.: Projected Change—Atmosphere. In: The BACC II Author Team (eds.). Second
640 Assessment of Climate Change for the Baltic Sea Basin. Regional Climate Studies, 217-234. Springer. DOI 10.1007/978-3-319-16006-1_102015 2015.

Christensen, O. B., and Kjellström, E.: Projections for Temperature, Precipitation, Wind, and Snow in the Baltic Sea Region until 2100. *Oxford Research Encyclopedia of Climate Science.* https://oxfordre.com/climatescience/view/10.1093/acrefore/9780190228620.001.0001/acrefore-9780190228620-e-695. DOI:
645 10.1093/acrefore/9780190228620.013.695, 2018.

Gröger M, Dieterich C, Meier HEM, Schimanke S.: Thermal air-sea coupling in hindcast simulations for the North Sea and Baltic Sea on the NW European shelf. Tellus A Dyn Meteorol Oceanogr 67(1):26911. doi: 10.3402/tellusa.v67.26911, 2015.

675    Gröger, M., Arneborg, L., Dieterich, C., Höglund, A., and Meier, H.E.M.: Summer hydrographic changes in the Baltic Sea, Kattegat and Skagerrak projected in an ensemble of climate scenarios downscaled with a coupled regional ocean–sea ice–atmosphere model. *Clim Dyn* **53,** 5945–5966 doi:10.1007/s00382-019-04908-9, 2019.

Gröger, M., Dieterich, C., and Meier, H. E. M.: Is interactive air sea coupling relevant for simulating the future climate of Europe?. *Clim Dyn*., 56, 491-514, https://doi.org/10.1007/s00382-020-05489-8, 2021a.

680    Gröger, M., Dieterich, C., Haapala, J., Ho-Hagemann, H. T. M., Hagemann, S., Jakacki, J., May, W., Meier, H. E. M., Miller, P. A., Rutgersson, A., and Wu, L. (2021b). Coupled regional Earth system modelling in the Baltic Sea region, Earth Syst. Dynam. Discuss. [preprint], https://doi.org/10.5194/esd-2021-14, in review, 2021.

Gustafsson N, Nyberg L and Omstedt A.: Coupling of a high-resolution atmospheric model and an ocean model for the Baltic Sea. Monthly Weather Review, 126, 2822– 2846, 1998.

685    Hagemann S, Machenhauer B, Jones R, Christensen OB, Deque M, Vidale PL.: Evaluation of water and energy budgets in regional climate models applied over Europe. Clim Dynam 23:547-567, 2004.

Hanel M, Buishand A.: Analysis of precipitation extremes in an ensemble of transient regional climate model simulations for the Rhine basin. Clim Dynam 36:1135-1153, 2011.

Held I, Soden B.: Robust response of the hydrological cycle to global warming. J Clim 19:5686-5699, 2006.

690    Ho-Hagemann HTM, Gröger M, Rockel B, Zahn M, Geyer B, Meier, HEM.: Effects of air-sea coupling over the North Sea and the Baltic Sea on simulated summer precipitation over Central EuropeClim Dyn 49: 3851. https://doi.org/10.1007/s00382-017-3546-8, 2017.

IPCC Climate Change 2001: The Scientific Basis. Contribution from Working Group I to the Third Assessment Report of the Intergovernmental Panel on Climate Change. Houghton JT, Ding Y, Griggs DJ, Noguer M, van der Linden PJ, Dai X, 695    Maskell K, Johnson CA (eds) Cambridge University Press, Cambridge, UK, 2001.

IPCC Climate Change 2007: The Physical Science Basis. Solomon S, Qin D, Manning M, Marquis M, Averyt K, Tignor MMB, Miller HL, Chen Z (eds), Cambridge University Press, Cambridge, UK Iversen T (2008) Preface. Tellus A 60(3):395-397, 2007.

IPCC Climate Change 2013: The Physical Science Basis. Contribution of Working Group I to the Fifth Assessment Report
700   of the Intergovernmental Panel on Climate Change [Stocker, T.F., D. Qin, G.-K. Plattner, M. Tignor, S.K. Allen, J.
Boschung, A. Nauels, Y. Xia, V. Bex and P.M. Midgley (eds.)]. Cambridge University Press, Cambridge, United Kingdom
and New York, NY, USA, 1535 pp, 2013.

Jacob, D., J. Petersen, B. Eggert, A. Alias, O. B. Christensen, L. M. Bouwer, A. Braun, A. Colette, M. Déqué, G.
Georgievski, E. Georgopoulou, A. Gobiet, L. Menut, G. Nikulin, A. Haensler, N. Hempelmann, C. Jones, K. Keuler, S.
705   Kovats, N. Kröner, S. Kotlarski, A. Kriegsmann, E. Martin, E. van Meijgaard, C. Moseley, S. Pfeifer, S. Preuschmann, C.
Radermacher, K. Radtke, D. Rechid, M. Rounsevell, P. Samuelsson, S. Somot, J.-F. Soussana, C. Teichmann, R. Valentini,
R. Vautard, B. Weber and Pascal Yiou:: EURO-CORDEX: new high-resolution climate change projections for European
impact research. *Regional Environmental Change.* doi: 10.1007/s10113-013-0499-2, 2013.

Kelemen, F.D., Primo, C., Feldmann, H., Ahrens, B.: Added Value of Atmosphere-Ocean Coupling in a Century-Long
710   Regional Climate Simulation, Atmosphere, 10(9), 537; https://doi.org/10.3390/atmos10090537, 2019.

Kendon, E, NM Roberts, HJ Fowler, MJ Roberts, SC Chan and CA Senior: Heavier summer downpours with climate change
revealed by weather forecast resolution model. Nature Climate Change 4, 570–576 doi:10.1038/nclimate2258, 2014.

Kjellström E.: Recent and future signatures of climate change in Europe. Ambio 33:193-198, 2004.

Kjellström E, and Ruosteenoja K.: Present-day and future precipitation in the Baltic Sea region as simulated in a suite of
715   regional climate models. Climatic Change. 81 (Suppl. 1), 281-291. doi:10007/s10584-006-9219-y, 2007.

Kjellström E, Bärring L, Jacob D, Jones R, Lenderink G, Schär C.: Modelling daily temperature extremes: Recent climate
and future changes over Europe. Climatic Change 81(S1):249-265, 2007.

Kjellström E, Lind P.: Changes in the water budget in the Baltic Sea drainage basin in future warmer climates as simulated
by the regional climate model RCA3. Boreal Environ Res 14:114-124, 2009.

720   Kjellström E, Nikulin G, Hansson U, Strandberg G, Ullerstig A.: 21st century changes in the European climate: uncertainties
derived from an ensemble of regional climate model simulations. Tellus A 63:24-40, 2011a.

Kjellström E, Räisänen J, Skaugen TE, Rögnvaldsson O, Agustsson H, Olafsson H, Nawri N, Björnsson H, Ylhäisi J,
Tietäväinen H, Gregow H, Jylhä K, Ruosteenoja K, Shkolnik I, Efimov S, Jokinen P, Benestad R.: Climate scenarios. In:
Thorsteinsson T, Björnsson H (eds). Climate Change and Energy Systems: Impacts, Risks and Adaptation in the Nordic and
725   Baltic countries. TemaNord 2011:502, 2011b.

Kjellström E, Thejll P, Rummukainen M, Christensen JH, Boberg F, Christensen OB, Fox Maule C.: Emerging regional climate change signals for Europe under varying large-scale circulation conditions. Clim Res 56:103-119, 2013.

Kjellström E, Bärring L, Nikulin G, Nilsson C, Persson G, and Strandberg G.: Production and use of regional climate model projections – a Swedish perspective on building climate services. Climate Services, 2-3, 15-29. Doi: 10.1016/j.cliser.2016.06.004, 2016.

Kjellström E, Nikulin G, Strandberg G, Christensen OB, Jacob D, Keuler K, Lenderink G, van Meijgaard E, Schär C, Somot S, Sørland SL, Teichmann C and Vautard R,: European climate change at global mean temperature increases of 1.5 and 2°C above pre-industrial conditions as simulated by the EURO-CORDEX regional climate models. Earth Syst. Dynam., 9, 459-478, DOI: 10.5194/esd-9-459-2018, 2018.

Kjellström E., Christensen O. B.: Regional Climate Modelling for the Baltic Sea Region. In: von Storch, H., (ed.). Climate of the Baltic Sea region. Oxford Research Encyclopedia of Climate Science. Oxford University Press USA. DOI: 10.1093/acrefore/9780190228620.013.700, 2020.

Kotlarski S, Keuler K, Christensen OB, Colette A, Déqué M, Gobiet A, Goergen K, Jacob D, Lüthi D, vanMeijgaard E, Nikulin G, Schär C, Teichmann C, Vautard R, Warrach-Sagi K, and Wulfmeyer V.: Regional climate modeling on European scales: a joint standard evaluation of the EURO-CORDEX RCM ensemble, Geosci. Model Dev., 7, 1297-1333, https://doi.org/10.5194/gmd-7-1297-2014, 2014.

Kyselý J, Gaál L, Beranová R, Plavcová E.: Climate change scenarios of precipitation extremes in Central Europe from ENSEMBLES regional climate models. Theor Appl Climatol 104:529-542, 2011.

Larsen AN, Gregersen IB, Christensen OB, Linde JJ, Mikkelsen PS.: Potential future increase in extreme one-hour precipitation events over Europe due to climate change. Water Sci Tech 60:2205-2216, 2009.

Lenderink G, van Meijgaard E.: Linking increases in hourly precipitation extremes to atmospheric temperature and moisture changes. Environ Res Lett 5:025208. doi:10.1088/1748-9326/5/2/025208, 2010.

Lenderink G, Belušić D, Fowler H, Kjellström E, Lind P, van Meijgaard E, van Ulft B and de Vries H.: Systematic increases in the thermodynamic response of hourly precipitation extremes in an idealized warming experiment with a convection-permitting climate model. Environ. Res. Lett. 14, 074012. DOI: 10.1088/1748-9326/ab214a, 2019.

Lind P, Kjellström E.: Temperature and precipitation changes in Sweden; a wide range of model-based projections for the 21st century. SMHI Reports Meteorology and Climatology, 113, 2008.

Lind, P., Belušić, D., Christensen, O.B. *et al.*: Benefits and added value of convection-permitting climate modeling over Fenno-Scandinavia. *Clim Dyn* **55,** 1893–1912 https://doi.org/10.1007/s00382-020-05359-3, 2020.

755    Meier HEM, Höglund A, Döscher R, Andersson H, Löptien U,Kjellström E.: Quality assessment of atmospheric surface fields over the Baltic Sea from an ensemble of regional climate model simulations with respect to ocean dynamics. Oceanologia 53:193-227, 2011.

Nakićenović, N., J. Alcamo, G. Davis, B. de Vries, J. Fenhann, S. Gaffin, K. Gregory, A. Grübler et al.: Emission scenarios. A Special Report of Working Group III of the Intergovernmental Panel on Climate Change. Cambridge University Press,
760    599 pp., 2000.

Nikulin G, Kjellström E, Hansson U, Jones C, Strandberg G, Ullerstig A.: Evaluation and future projections of temperature, precipitation and wind extremes over Europe in an ensemble of regional climate simulations. Tellus A 63:41-55, 2011.

Nilsen IB, Hanssen-Bauer I, Tveito OE, Wong WK.: Projected changes in days with zero crossings for Norway. Int J Climatol. 2021; 41: 2173– 2188. https://doi.org/10.1002/joc.6913, 2021.

765    Prein AF, Gobiet A, Truehetz H, Keuler K, Goergen K, Teichmann C, Fox Maule C, van Meijgaard E, Déqué M, Nikulin G, Vautard R, Colette A, Kjellström E and Jacob D.: Precipitation in the EURO-CORDEX 0.11˚ and 0.44˚ simulations: high resolution, high benefits? Clim. Dyn., doi: 10.1007/s00382-015-2589-y, 2015.

Primo, C., Kelemen, F. D., Feldmann, H., Ahrens, B.: A regional atmosphere-ocean climate system model (CCLMv5.0clm7-NEMOv3.3-NEMOv3.6) over Europe including three marginal seas: on its stability and performance, Geoscientific Model
770    Development Discussions, 2019, 1-33, doi:10.5194/gmd-2019-73, 2019.

Räisänen J.: Probabilistic projections of temperature and precipitation change for the period 2021- 2050, In: Proc. Future Climate and Renewable Energy: Impacts, Risks and Adaptation, 31 May - 2 June 2010, Oslo, p 78-79, 2010.

Räisänen, J., Eklund, J.: 21st century changes in snow climate in northern Europe: a high-resolution view from ENSEMBLES regional climate models. Clim Dynam 38:2575-2591, 2011.

775    Samuelsson P, Jones C, Willén U, Ullerstig A, Gollvik S, Hansson U, Kjellström E, Nikulin G, Wyser K.: The Rossby Centre Regional Climate Model RCA3: Model description and performance. Tellus A 63:4-23, 2011.

Schuler DV, Beldring S, Førland EJ, Roald LA, Engen-Skaugen T.: Snow cover and snow water equivalent in Norway: current conditions (1961-1990) and scenarios for the future (2071-2100). Met No Report no. 01/2006 Climate. Oslo, Norway, 2006.

780   Sein, D.V, Gröger, M., Cabos, W., Alvarez, F., Hagemann, S., de la Vara, A., Pinto, J.G., Izquierdo, A., Koldunov, N.V., Dvornikov, A. Y., Limareva, N., Martinez, B., Jacob, D.: Regionally coupled atmosphere - ocean - marine biogeochemistry model ROM: 2. Studying the climate change signal in the North Atlantic and Europe *J. Adv. Model. Earth Syst.*, https://doi.org/10.1029/2019MS001646 2020.

Seneviratne, S.I., N. Nicholls, D. Easterling, C.M. Goodess, S. Kanae, J. Kossin, Y. Luo, J. Marengo, K. McInnes, M.
785   Rahimi, M. Reichstein, A. Sorteberg, C. Vera, and X. Zhang,: Changes in climate extremes and their impacts on the natural physical environment. In: Managing the Risks of Extreme Events and Disasters to Advance Climate Change Adaptation [Field, C.B., V. Barros, T.F. Stocker, D. Qin, D.J. Dokken, K.L. Ebi, M.D. Mastrandrea, K.J. Mach, G.-K. Plattner, S.K. Allen, M. Tignor, and P.M. Midgley (eds.)]. A Special Report of Working Groups I and II of the Intergovernmental Panel on Climate Change (IPCC). Cambridge University Press, Cambridge, UK, and New York, NY, USA, pp. 109-230, 2012.

790   Strandberg G, Bärring L, Hansson U, Jansson C, Jones C, Kjellström E, Kolax M, Kupiainen M, Nikulin G, Samuelsson P, Ullerstig A and Wang S,: CORDEX scenarios for Europe from the Rossby Centre regional climate model RCA4. Reports Meteorology and Climatology, 116, SMHI, SE-60176 Norrköping, Sverige, 2014.

Taylor, KE, Stouffer, RJ, Meehl, GA.: An overview of CMIP5 and the experiment design. Bull. Am. Meteorol. Soc. 93, 485–498. http://dx.doi.org/ 10.1175/BAMS-D-11-00094.1, 2012.

795   Tobin I, Jerez S, Vautard R, Thais F, Déqué M, Kotlarski S, Maule CF, van Meijgaard E, Nikulin G, Noël T, Prein A & Teichmann C.: Climate change impacts on the power generation potential of a European mid-century wind farms scenario, Environmental Research Letters, 11, 034013, doi: 10.1088/1748-9326/11/3/034013, 2016.

van der Linden, P., and Mitchell, J. F. B., (eds): ENSEMBLES: climate change and its impacts: summary of research and results from the ENSEMBLES project. Met Office, Hadley Centre, Exeter, UK, 2009.

800   van Vuuren DP, Edmonds JA, Kainuma M, Riahi,K, Weyant J.: A special issue on the RCPs. Climatic Change 109:1-4, 2011.

Vautard R, Gobiet A, Sobolowski S, Kjellström E, Stegehuis A, Watkiss P, Mendlik T, Landgren O, Nikulin G, Teichmann C and Jacob D.: The European climate under a 2°C global warming. Environ. Res. Lett. 9, 034006, doi:10.1088/1748-9326/9/3/034006, 2014.

805   Vautard R, Kadygrov N, Iles C, Boberg F, Buonomo E, Bülow K, Coppola E, Corre L, van Meijgaard E, Nogherotto R, Sandstad M, Schwingshackl C, Somot S, Aalbers E, Christensen OB, Ciarlo JM, Demory M-E, Giorgi F, Jacob D, Jones RG, Keuler K, Kjellström E, Lenderink G, Levavasseur G, Nikulin G, Sillmann J, Solidoro C, Sørland SL, Steger C, Teichmann

C, Warrach-Sagi K and Wulfmeyer V.: Evaluation of the large EURO-CORDEX regional climate model ensemble. J. Geophys. Res. DOI: 10.1029/2019JD032344, 2020.

810 Wang S, Dieterich C, Döscher R, Höglund A, Hordoir R, Meier H, Samuelsson P and Schimanke S.: Development and evaluation of a new regional  coupled atmosphere ocean model in the North Sea  and Baltic Sea, Tellus A, 67, 24284. doi:10.3402/tellusa.v67.24284, 2015.

Wibig J., Mauran D., Benestad R., Kjellström E., Lorenz P., Christensen O. B.: Projected Change—Models and Methodology. In: The BACC II Author Team (eds.). Second Assessment of Climate Change for the Baltic Sea Basin.
815 Regional Climate Studies, 189-216. Springer. DOI 10.1007/978-3-319-16006-1_102015, 2015.

**Recommended Reading**

BACC II Author Team (2015) Second Assessment of Climate Change for the Baltic Sea Basin. Regional Climate Studies, Springer Verlag, Berlin, Heidelberg.